CHAPTER 4   8/28/2022
Planar Waves in Layered Media

The behavior of planar P- and S-waves in a layered elastic medium is one of the most useful (and mercifully one of the easiest) problems in seismology. There are many instances where the Earth can be approximated by plane layers and wave fronts are also approximately planar. As an added bonus, these problems can also provide useful insights into the dynamic behavior of buildings.

Unlike the last chapter in which there was no inherent coordinate frame for a homogeneous isotropic whole space, it is natural for the layered space problem to choose one of the coordinate axes to be perpendicular to the layering. In most cases it is customary to choose this to be the x_3 axis. If the waves are approximately planar, we can use Cartesian coordinates which simplifies the problem considerably. It is important to realize, though, that there is no physical situation in which truly planar waves exist. If a full solution is desired to the problem of a point source in a layered medium, then cylindrical coordinates are the best choice. However, the problem becomes much more complex.
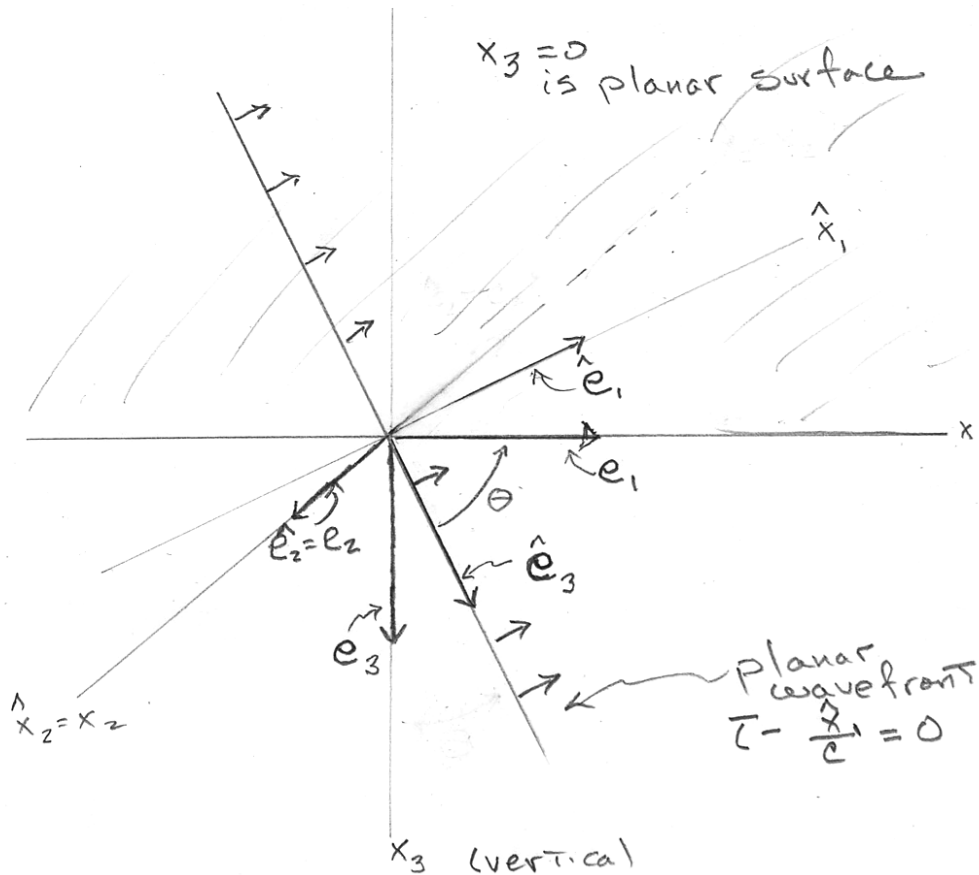

Figure 4.1. Natural Cartesian coordinate frames for planar waves in a layered medium

For the moment, let us consider Cartesian coordinate frames. There are two natural coordinate frames in the problem of planar waves in layered problems (see Figure 4.1). The first coordinate frame $(\hat{x}_1, \hat{x}_2, \hat{x}_3)$ is that used in Chapter 3 and it is defined by the planar wavefronts, with $\hat{\mathbf{e}}_1$ being in the direction of wave propagation. The second coordinate frame is natural to the layers with (x_1, x_2, x_3) perpendicular to the layering. In the Earth, we can choose $\mathbf{e}_3$ as either up or down (both are used … entropy of the universe increases). Because it is useful to have positive numbers for this coordinate and since the surface of the Earth at the top, it is most common to choose it as down. Now we choose $\hat{\mathbf{e}}_2 = \mathbf{e}_2$ to be the intersection of the plane of the layering with the plane of the wavefront. $\mathbf{e}_1$ is now defined to be perpendicular to $\mathbf{e}_2$ and $\mathbf{e}_3$, which is the projection of the propagation direction on the layering. Finally, $\hat{\mathbf{e}}_3$ is chosen to be perpendicular to both $\hat{\mathbf{e}}_1$ and $\hat{\mathbf{e}}_2$. θ is the angle between $\mathbf{e}_1$ and $\hat{\mathbf{e}}_3$ and it is usually referred to as the incidence angle; it is 0 degrees for a wavefront traveling perpendicular to the layering (a wave coming straight up). Using this coordinate frame, we see that planar P-waves can generally be written as

$$\mathbf{u}^P = f\left(t - \frac{\hat{x}_1}{\alpha}\right)\hat{\mathbf{e}}_1 \tag{4.1}$$

and shear waves can be generally written as

$$\mathbf{u}^S = \mathbf{u}^{SH} + \mathbf{u}^{SV} \tag{4.2}$$

where

$$\mathbf{u}^{SH} = f\left(t - \frac{\hat{x}_1}{\beta}\right)\hat{\mathbf{e}}_2 \tag{4.3}$$

and

$$\mathbf{u}^{SV} = g\left(t - \frac{\hat{x}_1}{\beta}\right)\hat{\mathbf{e}}_3 \tag{4.4}$$

Therefore, it is natural to decompose S-waves, whose particle motion is a 2-dimensional vector in the plane of the wavefront, into 1) the component that is horizontal (called the **SH wave**) and, 2) the component that has some vertical motion (called the **SV wave**). As before, f and g are independent functions with finite second derivatives.

When the source of the wave is a point, then the approximately planar waves are traveling radially away from the source, and we identify $\mathbf{e}_1, \mathbf{e}_2$, and $\mathbf{e}_3$ as the **radial, transverse, and vertical** directions, respectively.

Now the solutions (4.1), (4.3) and (4.4) are written in the $\hat{\mathbf{x}}$-coordinate frame. However, it is most convenient to write these solutions in the **x**-coordinate frame since the boundary conditions are more naturally described there. Now for the plane wave shown in Fig 4.1, which is traveling in the plus x_1 direction and the minus x_3 direction,

$$\mathbf{u}^P = f\left(t - p_\alpha x_1 + \eta_\alpha x_3\right)\left(\mathbf{e}_1 \sin\theta - \mathbf{e}_3 \cos\theta\right) \tag{4.5}$$

$$\mathbf{u}^{SV} = f\left(t - p_\beta x_1 + \eta_\beta x_3\right)\left(-\mathbf{e}_1 \cos\theta - \mathbf{e}_3 \sin\theta\right) \qquad (4.6)$$

$$\mathbf{u}^{SH} = f\left(t - p_\beta x_1 + \eta_\beta x_3\right)\mathbf{e}_2 \qquad (4.7)$$

where

$$p_\alpha = \frac{\sin\theta}{\alpha} \equiv \text{P-wave horizontal slowness} \equiv \text{P-wave ray parameter} \qquad (4.8)$$

$$p_\beta = \frac{\sin\theta}{\beta} \equiv \text{S-wave horizontal slowness} \equiv \text{S-wave ray parameter} \qquad (4.9)$$

$$\eta_\alpha = \frac{\cos\theta}{\alpha} \equiv \text{P-wave vertical slowness} \qquad (4.10)$$

$$\eta_\beta = \frac{\cos\theta}{\beta} \equiv \text{S-wave vertical slowness} \qquad (4.11)$$

SH-Waves in Two Welded Half-Spaces

The simplest problem of a plane wave in layered media is that of planar SH-waves in two welded half-spaces. The geometry of the problem is shown in Figure 4.3, a and b. I show the location of a traveling wavefront in part a, and in part b, I show an equivalent **ray diagram,** which is a shorthand from optics that shows the vector directions of the normal to wavefronts.

As in all of these problems, we have the correct solution when it 1) solves Navier's equation, 2) has continuous displacements on either side of the boundary, and 3) has equal and opposite traction vectors operating on either side of the boundary. In this simple problem it turns out that, except for certain incidence angles, it is possible to match these 3 conditions by the appropriate sum of three planar SH-waves, the **incident wave** in medium 1, the **reflected wave** in medium 1, and the **transmitted wave** in medium 2. As we have seen, planar SH-waves already solve Navier's equation. We can write the solution as

$$\mathbf{u}^1 = A_I f\left(t - px_1 + \eta_1 x_3\right)\mathbf{e}_2 + A_R f\left(t - px_1 - \eta x_3\right)\mathbf{e}_2 \qquad (4.12)$$

$$\mathbf{u}^2 = A_T f\left(t - px_1 + \eta_2 x_3\right)\mathbf{e}_2 \qquad (4.13)$$

"Wave fronts"

$A_2 M_2 \beta_2$

θ_T

x_1

θ_R

reflected wave front

θ_I

incident wave front

$P_1 M_1 \beta_1$

a)

$\sqrt{x_3}$

"Rays"

$A_2 M_2 \beta_2$

θ_T

Transmitted

x_1

incident ray

reflected

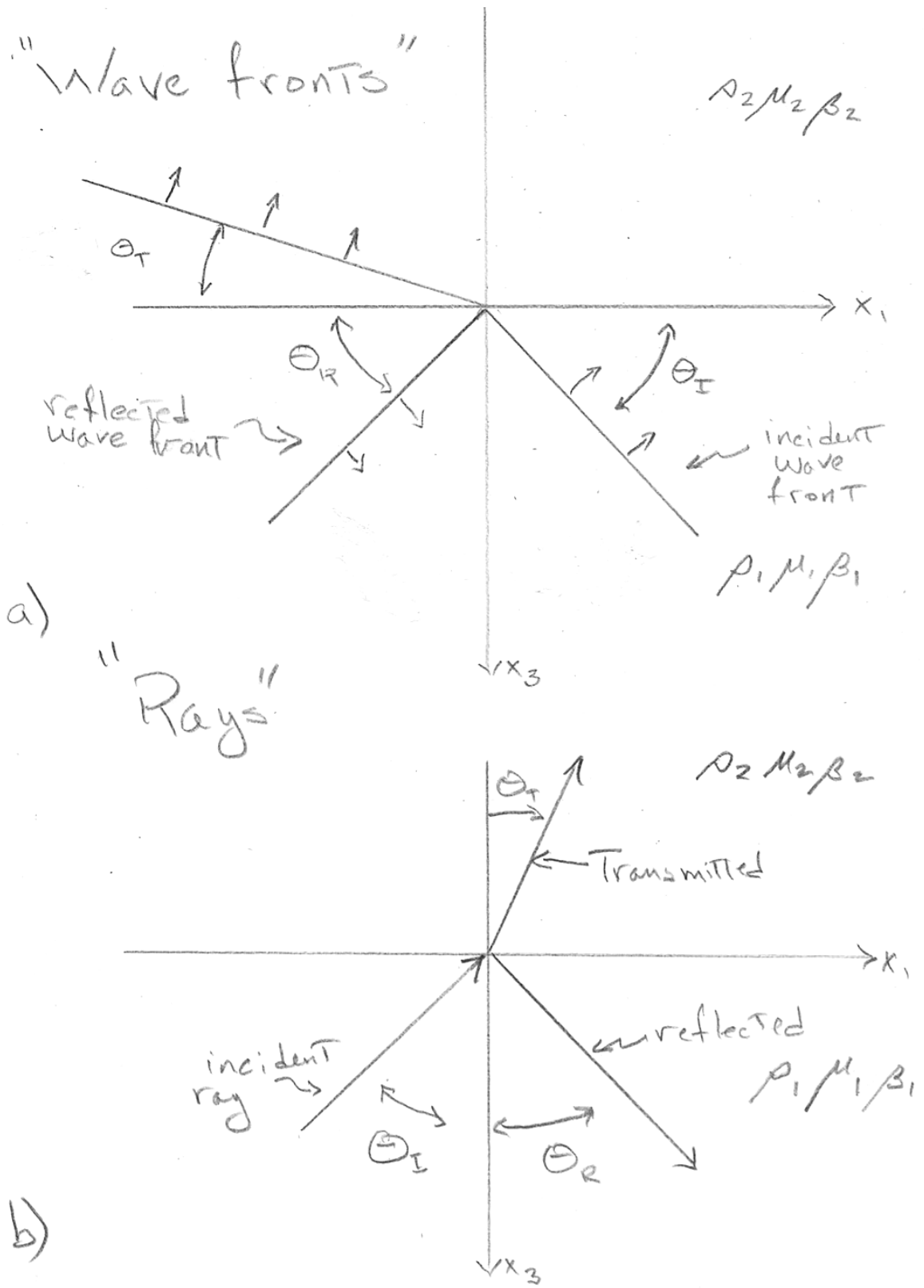$P_1 M_1 \beta_1$

θ_I

θ_R

b)

$\sqrt{x_3}$

Figure 4.2 SH plane wave from a faster to a slower medium

The requirement of continuous displacements on either side of the boundary can only occur if the planar wave fronts travel along the boundary at the same **apparent horizontal velocity** c. This is simply a statement of Snell's law. Since apparent velocities are infinite for vertically incident waves, seismologists sometimes use a parameter called slowness, which is defined to be the inverse of velocity. As it turns out for vertically layered problems, the apparent horizontal velocity of the wavefront (or **horizontal phase velocity)** is constant in the problem. The slowness of this horizontal phase velocity is called the **ray parameter**, p. By the same token, we can define a vertical phase velocity and its corresponding **vertical slowness** η, which is *not* the same in both media. That is

$$c = \frac{\beta_1}{\sin\theta_I} = \frac{\beta_1}{\sin\theta_R} = \frac{\beta_2}{\sin\theta_T} \tag{4.14}$$

$$p \equiv \frac{1}{c}, \quad \text{the same in both media} \tag{4.15}$$

$$\eta_1 = \frac{\cos\theta_I}{\beta_1} = \frac{\cos\theta_R}{\beta_1} \tag{4.16}$$

$$\eta_2 = \frac{\cos\theta_T}{\beta_2} \tag{4.17}$$

While (4.14) is a necessary condition for continuity of displacement, it is not sufficient. To solve the problem fully, we need to use the boundary condition that tractions at the interface are equal, which can be stated as

$$\sigma_{i3}^1\left(x, y, z = 0^+\right) = \sigma_{i3}^2\left(x, y, z = 0^+\right), \quad i = 1, 2, 3 \tag{4.18}$$

Because we have postulated a planar SH wave traveling in the x_1-direction, the only stress involved is σ_{23}, so

$$\sigma_{23}^1\left(x, y, z = 0^+\right) = \sigma_{23}^2\left(x, y, z = 0^+\right) \tag{4.19}$$

and

$$\sigma_{13}^1\left(x, y, z\right) = \sigma_{13}^2\left(x, y, z\right) = \sigma_{33}^1\left(x, y, z\right)\sigma_{33}^2\left(x, y, z\right) = 0 \tag{4.20}$$

It can be shown that condition (4.18), together with the continuity of displacement is satisfied if

$$\frac{A_R}{A_I} \equiv R_{SS}^{SH} = \frac{\mu_1\eta_1 - \mu_2\eta_2}{\mu_1\eta_1 + \mu_2\eta_2} = \frac{\mu_1\beta_2\cos\theta_1 - \mu_2\beta_1\cos\theta_2}{\mu_1\beta_2\cos\theta_1 + \mu_2\beta_1\cos\theta_2} \tag{4.21}$$

and

$$\frac{A_T}{A_I} \equiv T_{SS}^{SH} = \frac{2\mu_1\eta_1}{\mu_1\eta_1 + \mu_2\eta_2} = \frac{2\mu_1\beta_2}{\mu_1\beta_2\cos\theta_1 + \mu_2\beta_1\cos\theta} \tag{4.22}$$

R_{SS}^{SH} and T_{SS}^{SH} are called the reflection and transmission coefficients, respectively.

We can look at the special case of an SH plane wave that is reflecting off of a free surface. There is no transmitted wave in this case and the reflection coefficient is +1. This means that, at the free surface the incident and transmitted waves sum together in phase, or from (4.12) we conclude that

$$\mathbf{u}^{SH}\left(t; x_3 = 0\right) = 2A_I f\left(t - px_1\right)\mathbf{e}_2 \tag{4.23}$$

That is, the waves are twice as large at the free surface as they are inside the medium. Although the displacement is large, the stress is zero because of the free surface boundary condition.

The astute reader will note that this solution cannot make sense if the horizontal phase velocity of the incident wave is less than the shear-wave velocity in the transmitting medium; that is, β_2 is the minimum possible horizontal phase velocity in medium 2, and therefore if

$$c = \frac{\beta_1}{\sin\theta_1} < \beta_2 \tag{4.24}$$

then a purely plane wave solution is not possible. This is called a **post-critical reflection** and it turns out that the wave is totally reflected, but as we will see in a later chapter, the solution is fairly complex. $\theta_c = \sin^{-1}\left(\dfrac{\beta_1}{\beta_2}\right)$ is called the **critical angle**.

It is instructive to investigate the amplitude of the transmitted SH wave at vertical incidence, in which case (4.22) becomes

$$T_{SS}^{SH}\Big|_{\theta_1=0} = \frac{2\mu_1\beta_2}{\mu_1\beta_2 + \mu_2\beta_1} = \frac{2}{1 + \sqrt{\dfrac{\mu_2\rho_2}{\mu_1\rho_1}}} \tag{4.25}$$

Therefore, as the density times the rigidity of the transmitted medium becomes small, the amplitude of the transmitted wave can become twice as large as the incident wave. This may seem like a violation of conservation of energy, but it is not. Recall from equation (3.68) that energy flux is

$$P = \rho_2\beta_2\dot{u}_2^2 = \sqrt{\rho_2\mu_2}\,\dot{u}_2^2 \tag{4.26}$$

While the maximum amplitude of the transmitted wave is twice that of the incident wave, we can achieve even higher amplifications by transmitting the wave through a stack of smoothly decreasing velocity. In this case, there is very little reflection from each layer and most of the energy is transmitted through the entire medium. When this happens, the energy flux at the top is approximately that which is fed into the bottom. So for a **smooth velocity gradient**,

$$P_I \approx P_T \tag{4.27}$$

Or

$$u_2^T \approx u_2^I \sqrt{\frac{\rho_I \beta_I}{\rho_T \beta_T}} \tag{4.28}$$

where the indices T and I represent the material properties on the transmitted and incident sides of the gradient, respectively. Therefore, the transmitted wave can become very large in amplitude with respect to the incident wave.

P- and SV- Plane Waves

The problem gets far more complex when we consider either a P-wave or an SV-wave as the incident wave. The motion now involves two components of motion, which must be continuous on the boundary, and there are now two components of stress to match across the boundary.
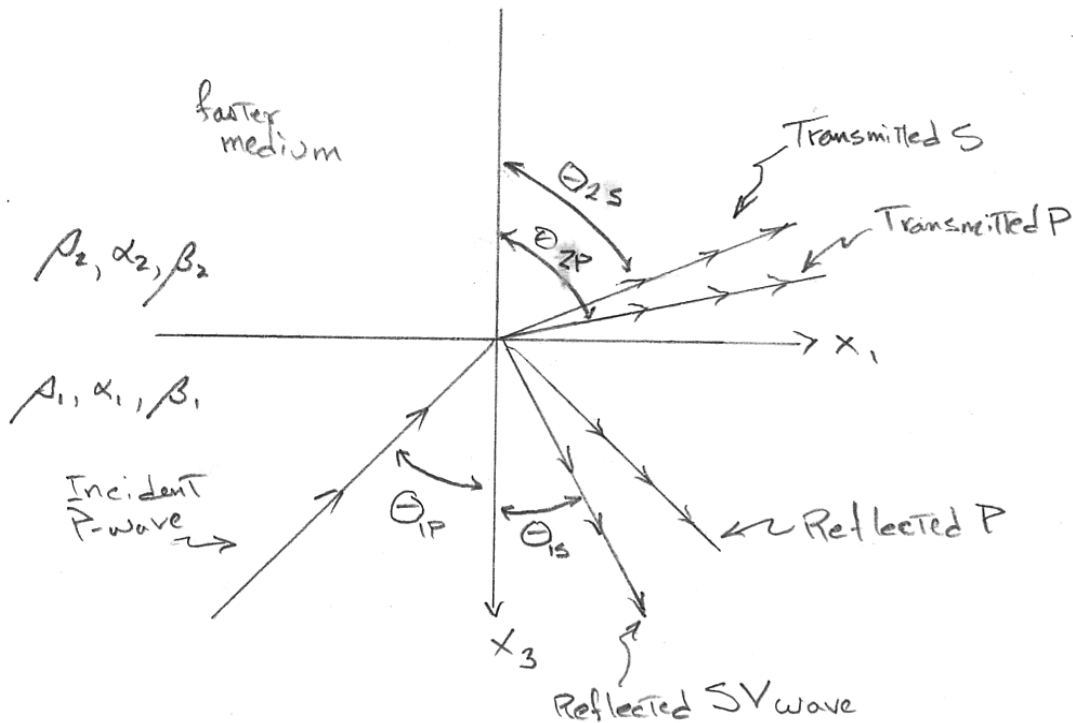
Figure 4.2 Ray diagram for a planar P-wave incident on a faster medium

Let us first consider the case of an incident planar P-wave. It turns out that the boundary conditions can be satisfied with the following superposition of plane waves. The ray diagram for these waves is shown in Figure 4.2.

$$\mathbf{u}^1 = A_{IP} f\left(t - px_1 + \eta_{\alpha_1} x_3\right)\left(\mathbf{e}_1 \sin\theta_{P1} + \mathbf{e}_3 \cos\theta_{P1}\right)$$

$$+ A_{IP} R_{PP} f\left(t - px_1 - \eta_{\alpha_1} x_3\right)\left(\mathbf{e}_1 \sin\theta_{P1} - \mathbf{e}_3 \cos\theta_{P1}\right) \quad (4.29)$$

$$+ A_{IP} R_{PS} f\left(t - px_1 - \eta_{\beta_1} x_3\right)\left(\mathbf{e}_1 \cos\theta_{S1} - \mathbf{e}_3 \sin\theta_{S1}\right)$$

The three terms represent incident P, reflected P, and reflected SV waves. The solution in medium 2 has the form

$$\mathbf{u}^2 = A_{IP} T_{PP} f\left(t - px_1 + \eta_{\alpha_2} x_3\right)\left(\mathbf{e}_1 \sin\theta_{P2} - \mathbf{e}_3 \cos\theta_{P2}\right)$$

$$+ A_{IP} T_{PS} f\left(t - px_1 + \eta_{\beta_2} x_3\right)\left(\mathbf{e}_1 \sin\theta_{S2} + \mathbf{e}_3 \cos\theta_{S2}\right) \quad (4.30)$$

As in the case of the SH wave, all of these wavefronts have identical horizontal phase velocities or

$$c = \frac{1}{p} = \frac{\alpha_1}{\sin\theta_{1P}} = \frac{\alpha_2}{\sin\theta_{2P}} = \frac{\beta_1}{\sin\theta_{1S}} = \frac{\beta_2}{\sin\theta_{2S}} \quad (4.31)$$

Two critical angles are now possible if

$$\theta_{cPP} = \sin^{-1}\left(\frac{\alpha_1}{\alpha_2}\right) \quad (4.32)$$

$$\theta_{cPS} = \sin^{-1}\left(\frac{\alpha_1}{\beta_2}\right) \quad (4.33)$$

The transmission and coefficients are derived in such a way that the following boundary conditions are satisfied. There are four non-zero boundary conditions for this problem

$$u_1^+ = u_1^- \quad (4.34)$$

$$u_3^+ = u_3^- \quad (4.35)$$

$$\sigma_{33}^+ = \sigma_{33}^- \quad (4.36)$$

$$\sigma_{13}^+ = \sigma_{13}^- \quad (4.37)$$

The following Table from Lay and Wallace gives the values of the reflection and transmission coefficients.

TABLE 3.1 Displacement Reflection and Transmission Coefficients

Coefficient	Formula
Solid–free surface (P–SV)	
R_{PP}	$\{-[(1/\beta^2) - 2p^2]^2 + 4p^2\eta_\alpha\eta_\beta\}/A$
R_{PS}	$\{4(\alpha/\beta)p\eta_\alpha[(1/\beta^2) - 2p^2]\}/A$
R_{SP}	$\{4(\beta/\alpha)p\eta_\beta[(1/\beta^2) - 2p^2]\}/A$
R_{SS}	$\{-[(1/\beta^2) - 2p^2]^2 + 4p^2\eta_\alpha\eta_\beta\}/A$
$R_{SS}(SH)$	1
Solid–solid (P–SV)	
R_{PP}	$[(b\eta_{\alpha_1} - c\eta_{\alpha_2})F - (a + d\eta_{\alpha_1}\eta_{\beta_2})Hp^2]/D$
R_{PS}	$-[2\eta_{\alpha_1}(ab + cd\eta_{\alpha_2}\eta_{\beta_2})p(\alpha_1/\beta_1)]/D$
T_{PP}	$[2\rho_1\eta_{\alpha_1}F(\alpha_1/\alpha_2)]/D$
T_{PS}	$[2\rho_1\eta_{\alpha_1}Hp(\alpha_1/\beta_2)]/D$
R_{SS}	$-[(b\eta_{\beta_1} - c\eta_{\beta_2})E - (a + b\eta_{\alpha_2}\eta_{\beta_1})Gp^2]/D$
R_{SP}	$-[2\eta_{\beta_1}(ab + cd\eta_{\alpha_2}\eta_{\beta_2})p(\beta_1/\alpha_1)]/D$
$R_{SS}(SH)$	$\dfrac{\mu_1\eta_{\beta_1} - \mu_2\eta_{\beta_2}}{\mu_1\eta_{\beta_1} + \mu_2\eta_{\beta_2}}$
$T_{SS}(SH)$	$\dfrac{2\mu_1\eta_{\beta_1}}{\mu_1\eta_{\beta_1} + \mu_2\eta_{\beta_2}}$

$a = \rho_2(1 - 2\beta_2^2 p^2) - \rho_1(1 - 2\beta_1^2 p^2)$ $\qquad E = b\eta_{\alpha_1} + c\eta_{\alpha_2}$

$b = \rho_2(1 - 2\beta_2^2 p^2) - 2\rho_1\beta_1^2 p^2$ $\qquad F = b\eta_{\beta_1} + c\eta_{\beta_2}$

$c = \rho_1(1 - 2\beta_1^2 p^2) + 2\rho_2\beta_2^2 p^2$ $\qquad G = a - d\eta_{\alpha_1}\eta_{\beta_2}$

$d = 2(\rho_2\beta_2^2 - \rho_1\beta_1^2)$ $\qquad H = a - d\eta_{\alpha_2}\eta_{\beta_1}$

$$D = EF + GHp^2$$

$$A = [(1/\beta^2) - 2p^2]^2 + 4p^2\eta_{\alpha_1}\eta_{\beta_1}$$

From Lay and Wallace

These coefficients are algebraically complex, and their behavior as a function of incidence angle is quite complex. Ewing, Jardetsky, and Press (Elastic Waves in Layered media) shows several plots of the behavior of these coefficients.
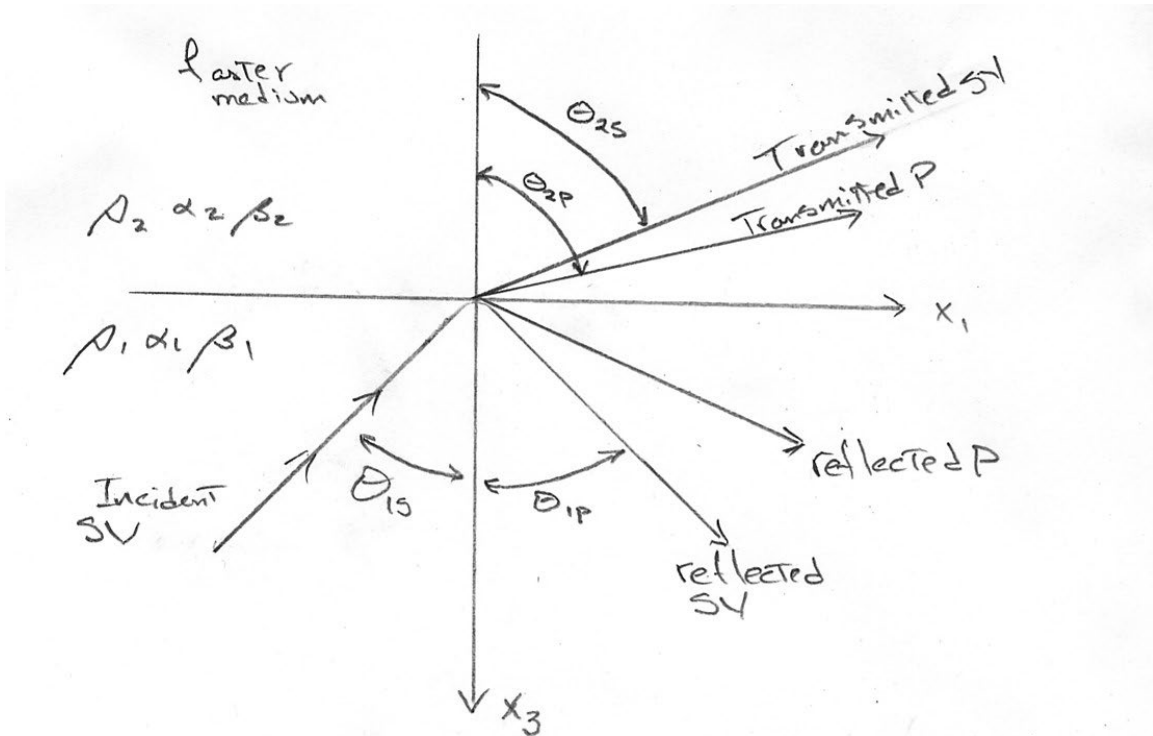
Figure 4.3 Ray diagram for a Planar SV wave incident on a faster medium.

The case for an **incident SV-wave** is very similar to the incident P-wave and the ray diagram for this case is shown in Figure 4.3. However, now there are as many as **three possible critical angles**, depending on the wave speeds. They can occur if

$$\theta_{cSS} = \sin^{-1}\left(\frac{\beta_1}{\beta_2}\right) \tag{4.38}$$

$$\theta_{cSP} = \sin^{-1}\left(\frac{\beta_1}{\alpha_2}\right) \tag{4.39}$$

$$\theta_{cSP} = \sin^{-1}\left(\frac{\beta_1}{\alpha_1}\right) \tag{4.40}$$

SH Waves in a Plate

We now address the problems of planar SH-waves in a plate. We will first solve the problem where both top and bottom surfaces are free, and then we will solve the problem where the bottom surface is fixed.

We begin with the problem where both the top and bottom surfaces are free. In this case there will be an infinite series of planar SH waves that are shown schematically in Figure 4.4. The boundary conditions are satisfied by the free surface reflection coefficient which, for SH waves is simply 1. To keep things simple, we restrict ourselves to looking at a single point on the free surface that we will set to be the origin.
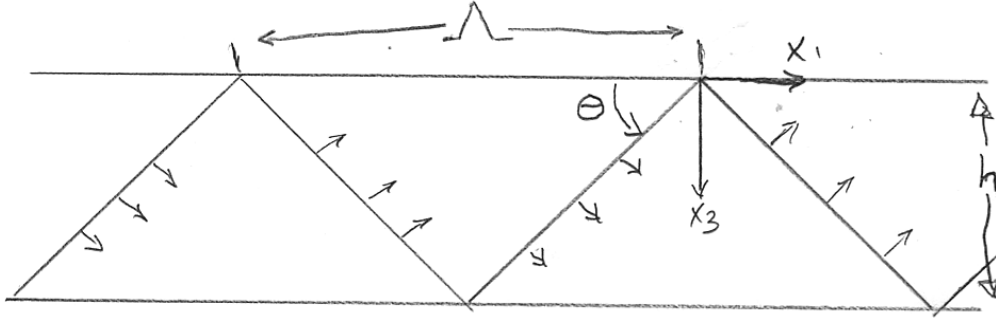
Figure 4.4. Geometry of a multiply reflecting SH-wave in a plate of thickness h.

In this case we can write the solution as

$$u_2\left(\mathbf{x}=\mathbf{0};t\right)=f\left(t\right)*\sum_{n=-\infty}^{\infty}\delta\left(t-nT\right)=f\left(t\right)*\mathrm{III}\left(\frac{t}{T}\right) \tag{4.41}$$

where III is called the **sampling function** (or sometimes called a comb function) and is defined as

$$\mathrm{III}\left(\frac{t}{T}\right)=\sum_{n=-\infty}^{\infty}\delta\left(t-nT\right) \tag{4.42}$$

The sampling function (and several other related functions) is shown in Figure 4.4.   The Fourier transform of a sampling function is also a sampling function (see Bracewell) and it is also shown in Figure 4.5. In this case

$$\mathrm{FT}\left[\mathrm{III}\left(\frac{t}{T}\right)\right]=T\mathrm{III}\left(\frac{T\omega}{2\pi}\right) \tag{4.43}$$

Therefore we can write the Fourier transform of the displacement as

$$\tilde{u}\left(\omega\right)=\tilde{f}\left(\omega\right)T\,\mathrm{III}\left(\frac{T\omega}{2\pi}\right)=T\sum_{n=-\infty}^{\infty}\tilde{f}\left(\omega_n\right) \tag{4.44}$$

for our purposes we will only consider non-negative values of n.

$$\omega_n=\frac{2\pi n}{T} \tag{4.45}$$

Therefore we see in (4.44) the solution just picks off discrete values of the Fourier transform of our function f. We can write the solution back in the time domain as

$$u\left(t\right)=T\sum_{n=-\infty}^{\infty}\left\{\mathrm{Re}\left[\tilde{f}\left(\omega_n\right)\right]\cos\left(\omega_n t\right)+\mathrm{Im}\left[\tilde{f}\left(\omega_n\right)\right]\sin\left(\omega_n t\right)\right\} \tag{4.46}$$

We call the discrete frequencies the **modes** of the solution. However, notice that these modes represent traveling waves except at vertical incidence. While they are modes, they are not normal modes.
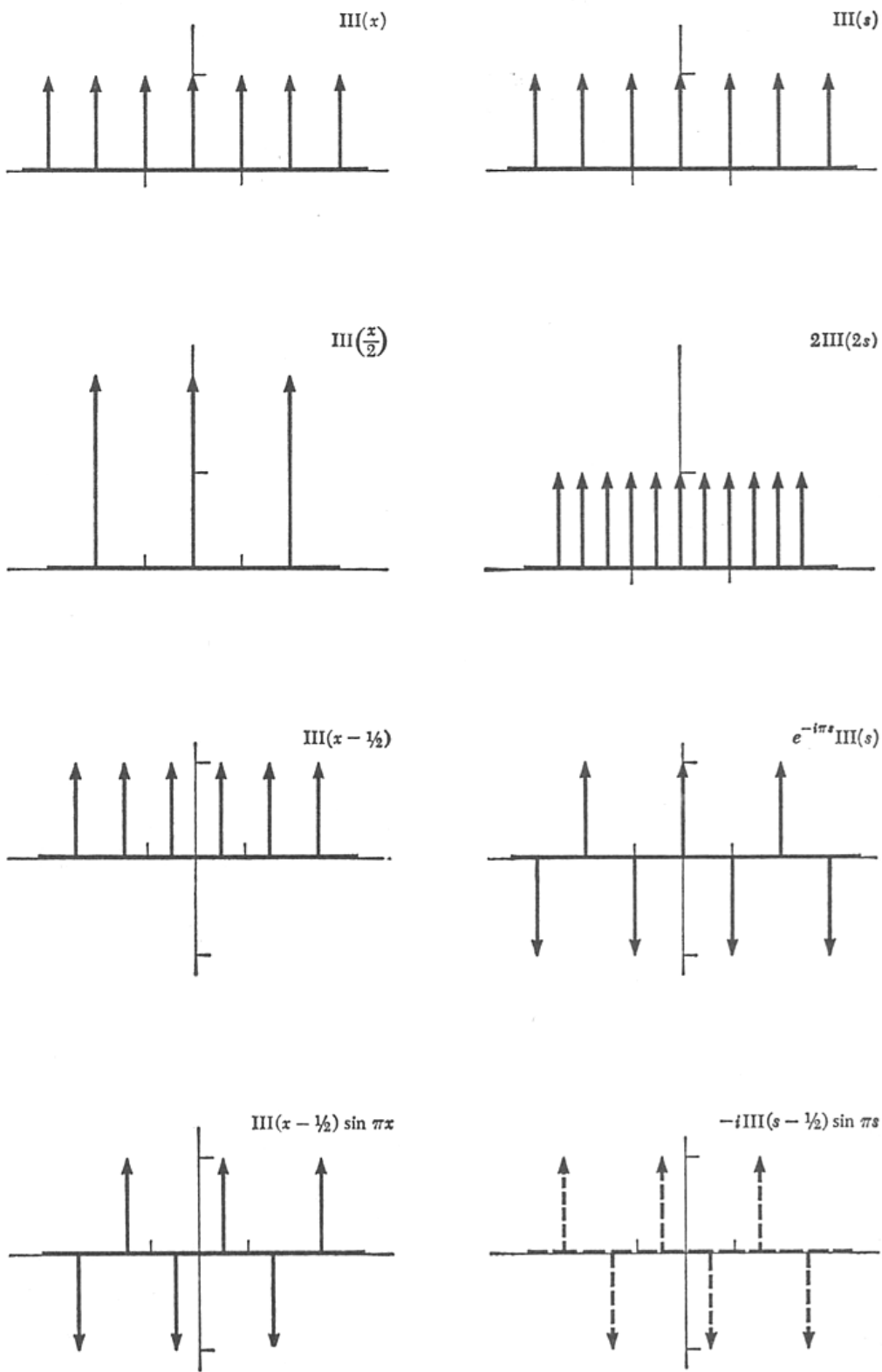
4-11

Figure 4.5 (from Bracewell, The Fourier Transform and its Applications). Notice that Bracewell uses the notation $\omega = 2\pi s$.

Recall though, that our original problem only specifies the thickness of the layer and T is still undetermined. From Figure 4.4 we see that

$$T = \frac{\Lambda}{c} \tag{4.47}$$

Where

$$c = \frac{\beta}{\sin\theta} \tag{4.48}$$

Now

$$\Lambda = \frac{2h}{\tan\theta} = 2h\frac{\cos\theta}{\sin\theta} = 2h\frac{\sqrt{1-\sin^2\theta}}{\sin\theta} = 2h\sqrt{\frac{1}{\sin^2\theta}-1} \tag{4.49}$$

substituting (4.48) into (4.49) gives

$$\frac{c^2}{\beta^2} = 1 + \left(\frac{\Lambda}{2h}\right)^2 \tag{4.50}$$

Therefore the horizontal phase velocity depends on the wavelength of the propagating wave. We can combine (4.45) and (4.47) to write

$$\Lambda = cT = 2\pi n\frac{c}{\omega_n} \tag{4.51}$$

substituting (4.51) into (4.50), and solving for c gives

$$c = \frac{\beta}{\sqrt{1-\left(\frac{n\pi\beta}{\omega_n h}\right)^2}} \tag{4.52}$$

We can interpret (4.52) in the following way. We can choose any mode number n and then we can choose any frequency ω_n and then we can use (4.52) to calculate the phase velocity. The phase velocity as a function of frequency is called the **dispersion curve** for the nth mode of the problem.

Notice that when the wave is traveling vertically $(\theta = 0)$ then both the phase velocity and the wavelength become infinite. However, we can still compute the modal frequencies for this case by recognizing that the periodicity of our sampling function in (4.41) is just twice the travel time through the layer or

$$T\Big|_{\theta=0} = \frac{2h}{\beta} \tag{4.53}$$

and then using (4.45) we see that

$$\omega_n\Big|_{\theta=0} = \frac{n\pi\beta}{h}; \quad n = 1, 2, 3, \ldots \tag{4.54}$$

where we have dropped the 0th mode, since it yields zero frequency and is not physically meaningful in this case. Notice that when there is a 0th mode, it corresponds to any horizontally traveling SH wave. The modes become true standing waves when the waves are traveling vertically.

We can also inquire what the full spatial solution looks like for each of these modes. That is, we assume that the time history is a cosine wave having a modal frequency and use (4.12) to write

$$\mathbf{u}^1 = \left\{ \cos\left[\omega_n\left(t - px_1 + \eta x_3\right)\right] + \cos\left[\omega_n\left(t - px_1 - \eta x_3\right)\right]\right\}\mathbf{e_2}$$
$$= 2\cos\left[\omega_n\left(t - px_1\right)\right]\cos\left(\omega_n\eta x_3\right)\mathbf{e_2}$$
(4.55)

Therefore we see that this is a cosine traveling with a particular phase velocity and with a depth dependence that is a fixed cosine function. We can now recognize that the vertical mode shapes must be such that the shear stress and shear strain are zero at the boundaries of the plate, or

$$\sigma_{23}\Big|_{x_3=0} = \mu\varepsilon_{23}\Big|_{x_3=0} = 0 \tag{4.56}$$

$$\sigma_{23}\Big|_{x_3=h} = \mu\varepsilon_{23}\Big|_{x_3=h} = 0 \tag{4.57}$$

This must mean that

$$\varepsilon_{23}\Big|_{x_3=0,h} = \frac{\partial u_2}{\partial x_3}\Big|_{x_3=0,h} = -2\omega_n\eta\cos\left[\omega_n\left(t - px_1\right)\right]\sin\left(\omega_n\eta x_3\right)\Big|_{x_3=0,h} = 0 \tag{4.58}$$

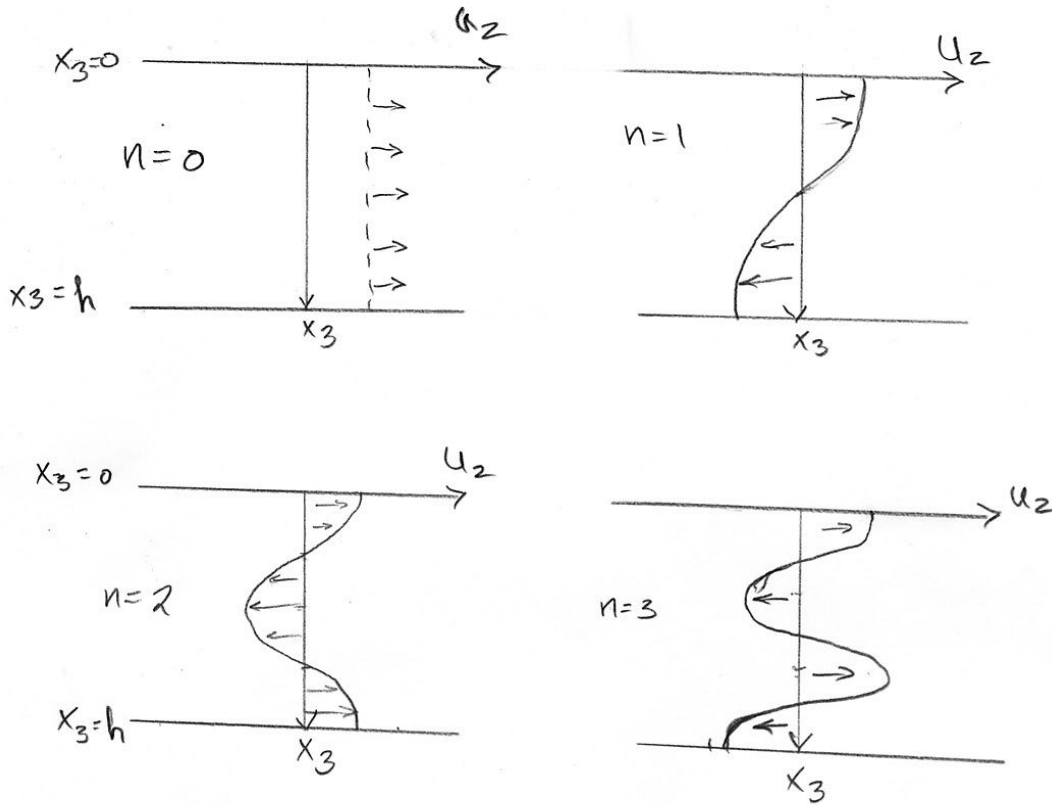This condition is only satisfied if the vertical distribution of the displacement has the forms shown in Figure 4.5.

Figure 4.5. Depth dependence of horizontal displacement for the first 4 modes of harmonic SH-waves in a plate with free boundaries.

Planar SH-waves in a Plate with a Rigid Base

While the free plate problem is simple and useful to show modes and dispersion, a more important problem for us is one in which the base of the plate is fixed to a rigid medium. This problem is identical to the free-boundary problem, except that the reflection coefficient at the bottom of the layer is -1 instead of +1. That is, the up- and down-going waves in Figure 4.3 destructively interfere at the bottom of the layer so that there is no displacement here. If the plane waves are impulse functions, then the ground motion at the origin is now an alternating series of positive and negative impulses as given by

$$u_2\left(\mathbf{x}=\mathbf{0};t\right)=f\left(t\right)*\sum_{n=-\infty}^{\infty}\left[\delta\left(t-nt\right)\right]-\delta\left(t-\frac{T}{2}-nT\right)$$

$$=f\left(t\right)*\left[\mathrm{III}\left(\frac{t}{T}\right)-\mathrm{III}\left(\frac{t}{T}-\frac{1}{2}\right)\right]=f\left(t\right)*\mathrm{III}\left(\frac{t}{T}-\frac{1}{2}\right)\sin\left(\frac{\pi t}{T}\right)$$

(4.59)

Figure 4.4 shows the Fourier transform of this alternating comb function (the bottom function in the figure) is also an alternating comb function, which can be written

$$FT\left[\mathrm{III}\left(\frac{t}{T}-\frac{1}{2}\right)\sin\left(\frac{\pi t}{T}\right)\right]=-iT\,\mathrm{III}\left(\frac{T\omega}{2\pi}-\frac{1}{2}\right)\sin\left(\frac{T\omega}{2}\right)$$

(4.60)

This solution is very similar to the free plate solution, except the frequencies of the modes have been changed. There is no mode for $n = 0$, since that corresponds to uniform horizontal motion with depth, which cannot be possible if the motion at the bottom is zero. The modal frequencies are given by

$$\omega_n = \frac{\pi(2n-1)}{T}; \qquad n = 1, 2, 3, \ldots \tag{4.61}$$

In this case the alternating comb function repeats itself only every other reflection, and so in this case

$$T = \frac{2\Lambda}{c} \tag{4.62}$$

where Λ is the same as shown in Figure 4.4, and as before

$$c = \frac{\beta}{\sin\theta} \tag{4.63}$$

Just as before,

$$\frac{c^2}{\beta^2} = 1 + \left(\frac{\Lambda}{2h}\right)^2 \tag{4.64}$$

However, in this case,

$$2\Lambda = cT = 2\pi n \frac{c}{\omega_n} \tag{4.65}$$

Therefore, the horizontal phase velocity is

$$c = \frac{\beta}{\sqrt{1 - \left(\dfrac{n\pi\beta}{2\omega_n h}\right)^2}} \tag{4.66}$$

As before, if the wavefront is vertically incident, the phase velocity become infinite, and the interfering waves form a true standing wave with

$$T\Big|_{\theta=0} = \frac{4h}{\beta} \tag{4.67}$$

And

$$\omega_n\Big|_{\theta=0} = \frac{(2n-1)\pi\beta}{2h}; \qquad n = 1, 2, 3, \ldots \tag{4.68}$$
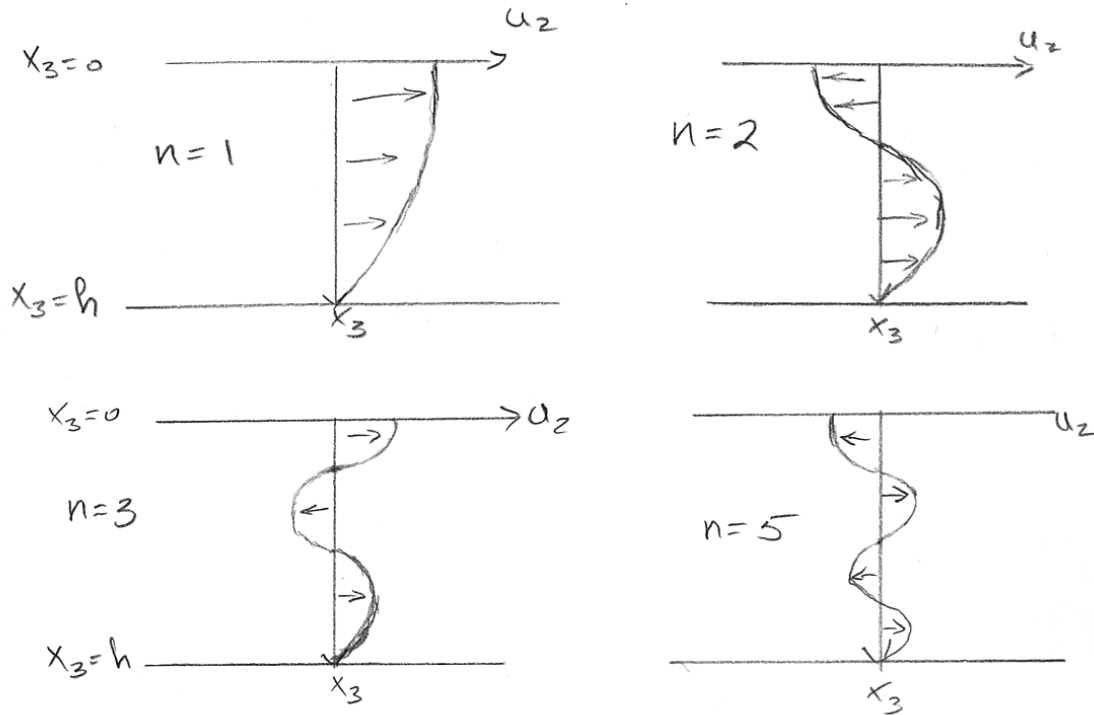
Figure 4.6. Amplitude as a function of depth for the first 4 SH modes of a plate with a fixed bottom and a free surface at the top.

We can now compute the mode shape by noting that we must now add both positive and negative waves that are shifted by a quarter wavelength, so that

$$
\begin{aligned}
\mathbf{u}^1 &= \cos\left[\omega_n\left(t - px_1 + \eta x_3\right)\right]\mathbf{e_2} + \cos\left[\omega_n\left(t - px_1 - \eta x_3\right)\right]\mathbf{e_2} \\
&\quad - \sin\left[\omega_n\left(t - px_1 + \eta x_3\right)\right]\mathbf{e_2} - \sin\left[\omega_n\left(t - px_1 - \eta x_3\right)\right]\mathbf{e_2} \\
&= 2\cos\left[\omega_n\left(t - px_1\right)\right]\cos\left(\omega_n\eta x_3\right)\mathbf{e_2} - 2\sin\left[\omega_n\left(t - px_1\right)\right]\cos\left(\omega_n\eta x_3\right)\mathbf{e_2} \qquad (4.69) \\
&= 2\cos\left(\omega_n\eta x_3\right)\left\{\cos\left[\omega_n\left(t - px_1\right)\right] - \sin\left[\omega_n\left(t - px_1\right)\right]\right\}\mathbf{e_2} \\
&= 2\sqrt{2}\cos\left(\omega_n\eta x_3\right)\cos\left[\omega_n\left(t - px_1\right) - \frac{\pi}{4}\right]\mathbf{e_2}
\end{aligned}
$$

So we end up with a sum of a sinusoid and a cosine in the x_1 direction, and our familiar cosine in the vertical direction. Because there are different natural frequencies, the mode shapes are different as is shown in Figure 4.6. Notice that the displacement is zero at the bottom boundary, but the strain (derivative of displacement with respect to vertical position) is zero at the top.

Comparing Figures 4.5 and 4.6, it is easy to see why free plates have mode frequencies that are integer multiples of the fundamental mode, whereas a plate with one fixed

boundary has modal frequencies that are odd integer multiples of the fundamental mode frequency.

Phase Velocity and Group Velocity

We have seen that planar plate waves have horizontal phase velocities $c = \dfrac{1}{p}$ that vary with the frequency of the motion, or alternatively with the wavelength of the waves. In particular, we can write them in generalized form as

$$u_2 = g(x_3)\sin\left[\omega\left(t - \frac{x_1}{c}\right)\right]$$
$$= g(x_3)\sin(\omega t - kx_1)$$

(4.70)

where $g(x_3)$ is a harmonic function of depth and $c = \dfrac{\Lambda}{T} = \dfrac{\omega}{k}$, and k is the horizontal spatial frequency which is commonly referred to as horizontal wavenumber. That is for a harmonic traveling wave, the phase velocity can always be measured by taking the frequency divided by the appropriate wavenumber. Remember, though, this is just the apparent velocity of some particular phase in the harmonic wave. Since harmonic waves have no beginning or end, they do not carry any information. In order to carry information (or energy) the wave must vary in time and space; it must be possible to follow a wave packet. The easiest way to understand a wave packet is to consider the case of two harmonic waves of similar (but different) frequencies. That is, consider

$$u_2(x_1, t) = A_0 \cos(\omega_1 t - k_1 x_1) + A_0 \cos(\omega_2 t - k_2 x_1)$$
$$= 2A_0 \cos\left(\frac{\omega_1 - \omega_2}{2}t - \frac{k_1 - k_2}{2}x_1\right)\cos\left(\frac{\omega_1 + \omega_2}{2}t - \frac{k_1 + k_2}{2}x_1\right)$$
$$= u_{group}u_{carrier}$$

(4.71)

Where $u_{carrier}$ is the sinusoid with the average frequency of the signals and it's frequency is that of the "carrier signal." The two signals beat against each other and the beat frequency is the difference in frequencies of the two signals. Of course, there are similar carrier and beat wavenumbers. As before the *phase velocity of the carrier* is just

$$c_{carrier} = \frac{\omega_{carrier}}{k_{carrier}} = \frac{\omega_1 + \omega_2}{k_1 + k_2}$$

(4.72)

And the *group velocity* of the amplitude envelope is just

$$c_{group} = \frac{\omega_{group}}{k_{group}} = \frac{\omega_1 - \omega_2}{k_1 - k_2} = \frac{\Delta\omega}{\Delta k} \approx \frac{d\omega}{dk}$$

(4.73)

The wavegroup carries energy and information and its speed must not exceed the intrinsic velocity of the medium. The phase velocity can be any number higher than the intrinsic wave velocity. If you know $\omega(k)$, then you can always obtain the group velocity by differentiating with respect to k. For example, if we return the problem of a plane wave in a plate, the phase velocity is given by (4.52), or

4-18

$$c_{carrier} = \frac{\omega_n}{k} = \frac{\beta}{\sqrt{1 - \left(\frac{n\pi\beta}{\omega_n h}\right)^2}} \tag{4.74}$$

Or

$$\omega_n = \frac{\beta}{h}\sqrt{k^2 h^2 + n^2 \pi^2} \tag{4.75}$$

So

$$c_{group} = \frac{d\omega_n}{dk} = \beta h \frac{k}{\sqrt{k^2 h^2 + n^2 \pi^2}} \tag{4.76}$$

Or we can infer the group velocity as a function of ω by noting that $k = \dfrac{\omega_n}{c_{carrier}}$, so that (4.76) becomes

$$c_{group} = \frac{\beta h \omega_n}{c_{carrier}\sqrt{\omega_n^2 \frac{h^2}{c_{carrier}^2} + n^2 \pi^2}} \tag{4.77}$$

Substituting (4.74) into (4.77), we obtain

$$c_{group} = \frac{\beta h \omega_n}{\dfrac{\beta}{\sqrt{1 - \left(\dfrac{n\pi\beta}{\omega_n h}\right)^2}}\sqrt{\omega_n^2 \dfrac{\dfrac{h^2}{\beta^2}}{1 - \left(\dfrac{n\pi\beta}{\omega_n h}\right)^2} + n^2 \pi^2}}$$

$$\tag{4.78}$$

$$= \beta \frac{1}{\sqrt{1 + \dfrac{n^2 \pi^2 \beta^2}{\left(\omega_n^2 h^2 - n^2 \pi^2 \beta^2\right)}}}$$

Planar SH-Waves in Layered Media

The problem of horizontally-polarized S-waves in a vertically stratified space is one of the most fundamental problems in Engineering Seismology. This is primarily because of the large changes in seismic velocity near the Earth's surface. That is, seismic velocities generally increase dramatically with depth as overburden pressures increase. There can also be large velocity contrasts at the water table. Furthermore, the seismic velocity of loosely consolidated sediments can be much lower than that of crystalline rock. Since the

average S-wave velocity at the typical depth of earthquakes is 3.5 km/sec, most shear-waves are traveling nearly vertically as they propagate through the upper 100 meters of the Earth. For near-vertical incidence, there is little distinction between SV and SH; they are both nearly horizontally polarized. Therefore, it is of great interest to investigate how a horizontally polarized S-wave propagates through a series of horizontal layers.

The following Figures are from "Borehole velocity measurements and geological conditions at thirteen sites in the Los Angeles, Californis, region," by Gibbs, Tinsely, Boore, and Joyner (USGS Open File Report 00-470). They provide a good idea of the nature of near-surface seismic velocities encountered at real-world construction sites.
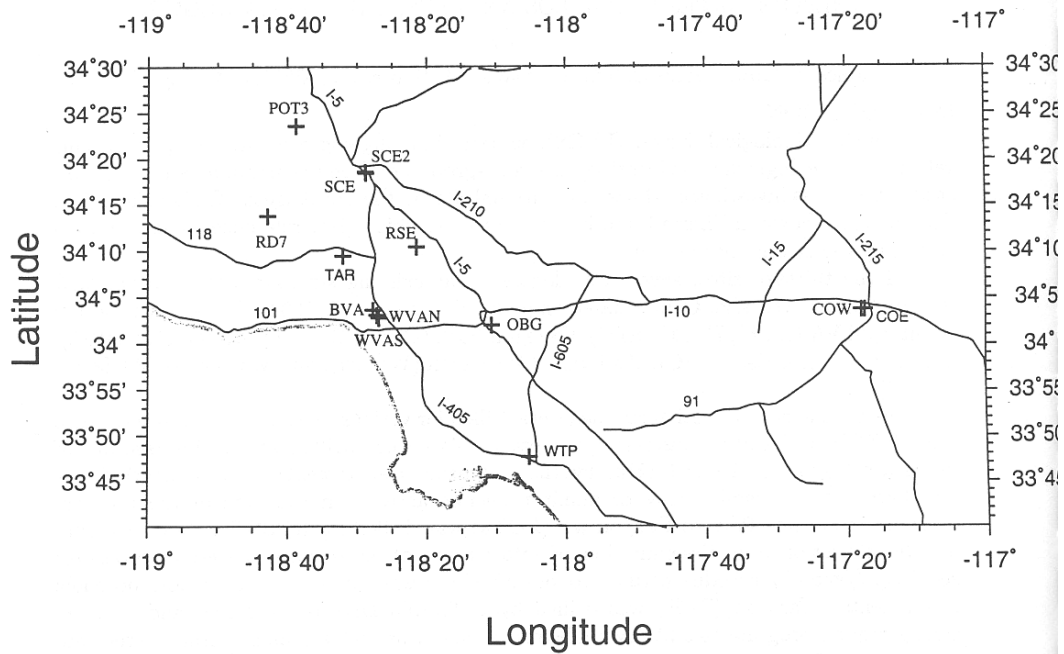
Figure 4.7 Locations of boreholes for velocity profiles shown in following figures
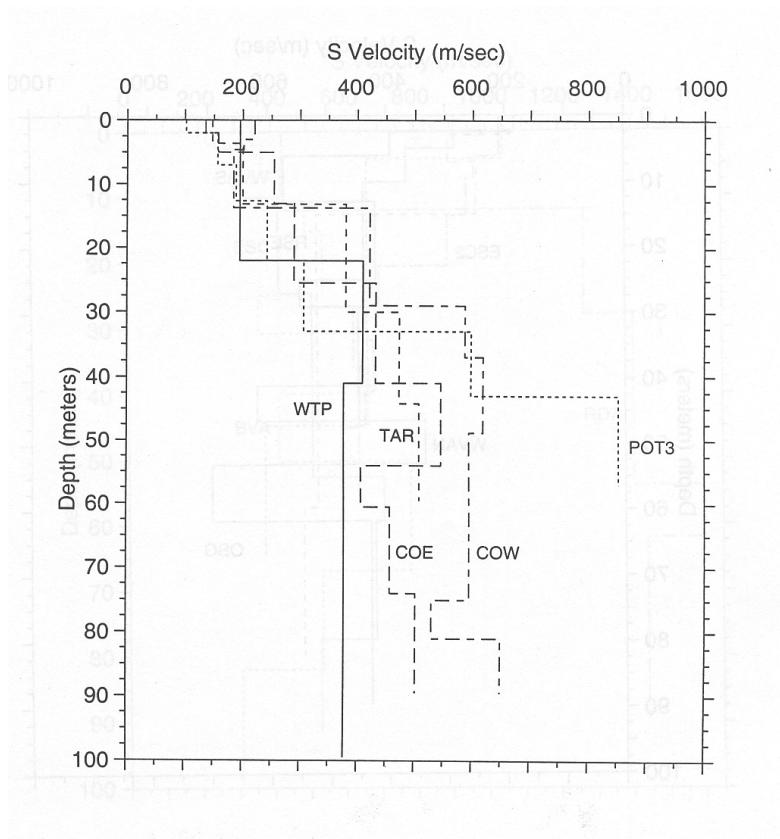
Figure 4.8 Shear-wave velocities for boreholes at stations shown in Figure 4.7
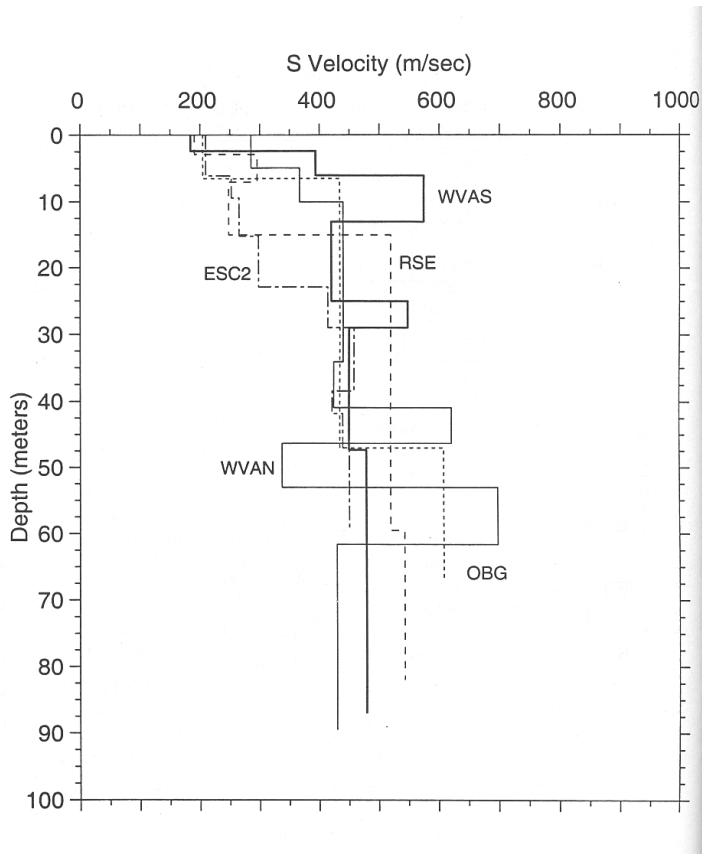
Figure 4.9 and 4.10 Shear-wave velocities for boreholes at stations shown in Figure 4.7
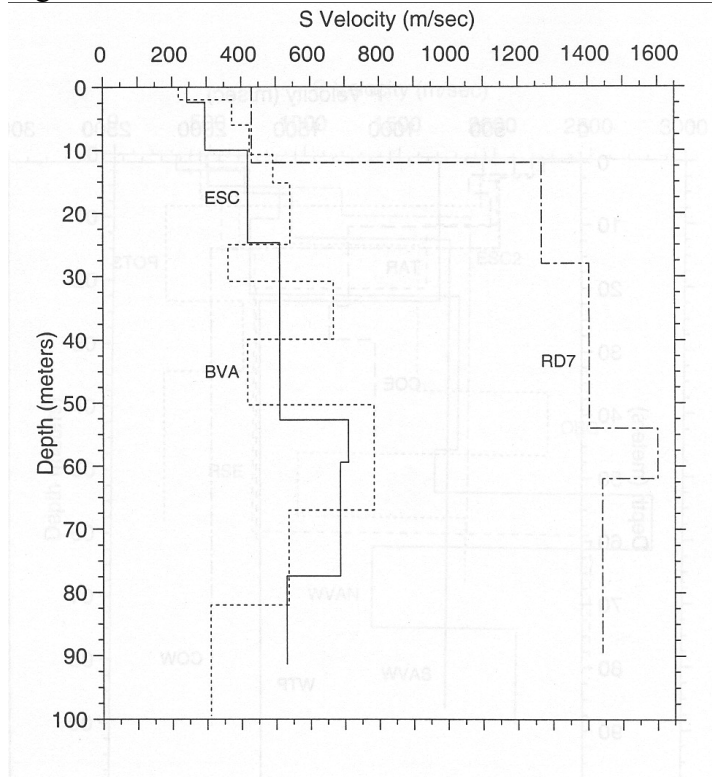
Thompson (Transmission of elastic waves through a stratified solid medium, J. Appl. Phys., 21, 89-93, 1950) and Haskell (The dispersion of surface waves on multi-layered media, Bull. Seism. Soc. Am., 43, 17-34, 1953) describe a clever method for solving the problem of a harmonic planar P-, SV-, or SH-wave through a vertically stratified medium. The algebra of the problem is beyond the scope of these notes, but I will sketch out the solution for a planar harmonic SH-wave. The methodology is known as **Thompson-Haskell Propagator Matrices** and it is the basis of a widely used computer program known as **Shake**. The following is a modification of Haskell's classic paper, "Crustal reflection of plane SH-waves" (JGR, 1960, 4147-4150).
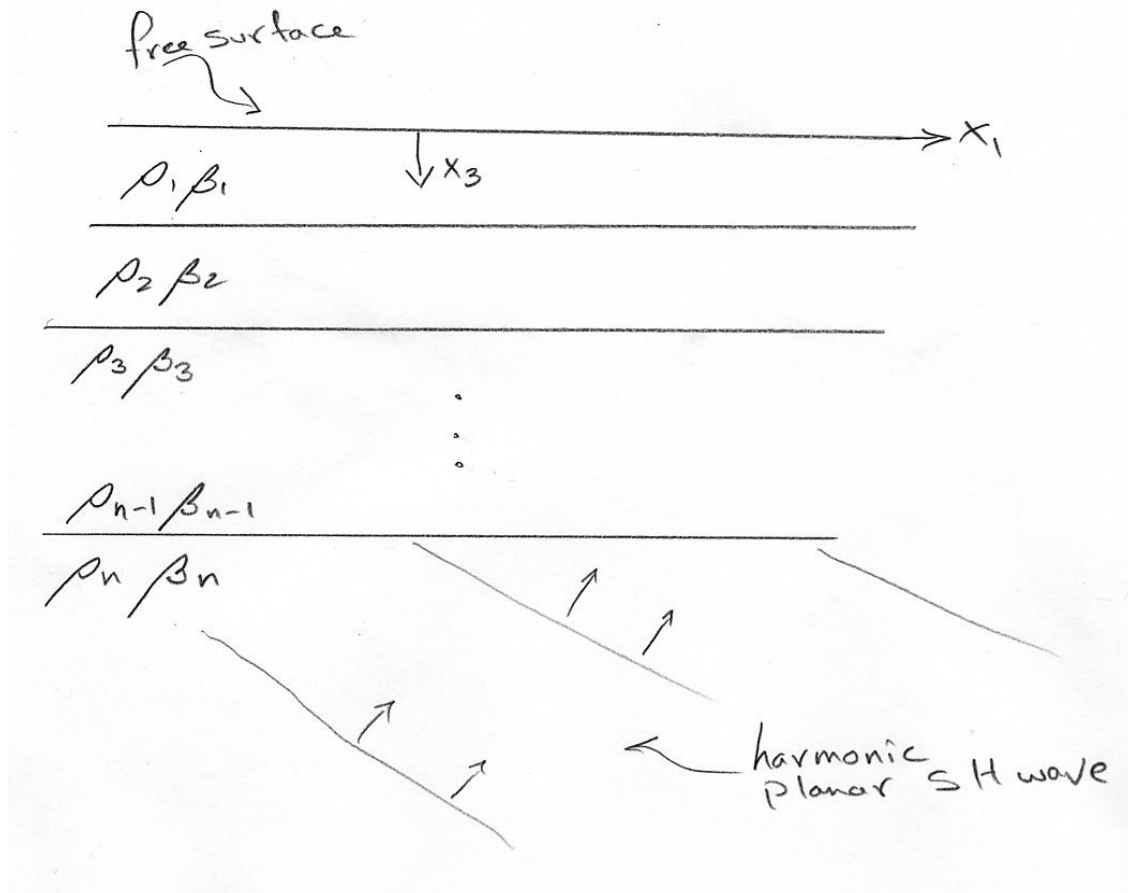
Figure 4.11

Consider the stack of *n-1* plane layers over an elastic half space with a planar SH-wave incident from the half-space as is shown in Figure 4.11. We will consider that the plane wave is harmonic, although this requirement can be relaxed later, since we can sum harmonic solutions to form the solution for any time history for the incident wave. Motivated by the solutions for a planar SH-wave in a plate, we recognize that solutions to our problem will have some part that travels horizontally at the same phase velocity throughout the medium and another part of the solution that describes the depth dependence of the motion. That is, the solution will be of the form

$$\mathbf{u} = g(x_3)\cos\left[\omega(t - px_1) - \delta\right]\mathbf{e_2} \tag{4.79}$$

where $g(x_3)$ is a function of depth that will allow us to match the appropriate boundary conditions, and δ is a phase lag that may also be a function of depth.

At each boundary, there are two important conditions, continuous displacement and stress. Thompson and Haskell devised a clever solution method that writes these boundary conditions in matrix form. If we denote the amplitude of the up-going SH wave incident at the bottom of the stack as g^I, then the amplitude at the surface of the Earth g^0 can be written as

$$g^0 = g^I \left(\frac{2\mu_n \gamma_n}{\mu_n \gamma_n A_{11} + A_{21}} \right) \tag{4.80}$$

Where

$$\gamma_n \equiv \sqrt{\frac{c^2}{\beta_n^2} - 1} \tag{4.81}$$

And

$$A = \prod_{m=n-1}^{1} a_m = a_{n-1} a_{n-2} a_{n-2} .. a_1 \tag{4.82}$$

And

$$a_m = \begin{bmatrix} \cos Q_m & i\left(\mu_m \gamma_m\right)^{-1} \sin Q_m \\ i\left(\mu_m \gamma_m\right)^{-1} \sin Q_m & \cos Q_m \end{bmatrix} \tag{4.83}$$

And

$$Q_m = \frac{\omega h_m \gamma_m}{c} = \omega h_m \sqrt{\frac{1}{\beta_m^2} - \frac{1}{c^2}} \tag{4.84}$$

Unfortunately, these equations become singular for vertical incidence. That is, at vertical incidence, the horizontal phase velocity becomes infinite in which case,

$$\gamma_m \Big|_{c \to \infty} = \frac{c}{\beta} \tag{4.85}$$

$$Q_m \Big|_{c \to \infty} = \frac{\omega h_m}{\beta_m} \tag{4.86}$$

and then

$$a_m \Big|_{c \to \infty} = \begin{bmatrix} \cos\left(\omega h_m \beta_m^{-1}\right) & 0 \\ 0 & \cos\left(\omega h_m \beta_m^{-1}\right) \end{bmatrix} \tag{4.87}$$

Thus, $a_{21} \to 0$ at vertical incidence.

We can gain some insight by considering the simple case of a single layer over a half space. In this case, $n = 2$ and we need only consider one propagator matrix. Therefore,

$$A_{11} \cos Q_1 \tag{4.88}$$

$$A_{21} = i\left(\mu_1\gamma_1\right)^{-1}\sin Q_1 \tag{4.89}$$

And

$$g^0 = g^I\left(\frac{2}{\cos Q_1 + ib\sin Q_1}\right) \tag{4.90}$$

Where

$$b = \frac{\mu_1\gamma_1}{\mu_2\gamma_2} \tag{4.91}$$

we can write the amplitude of the amplification as

$$\left|\frac{g^0}{g^I}\right|^2 = \frac{2}{\cos^2 Q_1 + b\sin^2 Q_1} = \frac{2}{1 + (b-1)\sin^2 Q_1} \tag{4.92}$$

The nature of the amplification depends on whether or not b is greater than 1. Let c_1 be the phase velocity for which $b = 1$, then

$$c_1^2 = \frac{\rho_2^2\beta_2^4 - \rho_1^2\beta_1^4}{\rho_2^2\beta_2^2 - \rho_1^2\beta_1^2} \tag{4.93}$$

If $c > c_1$, then $b < 1$ and the maxima of $\left|\dfrac{g^0}{g^I}\right|$ occur at frequencies given by $\cos Q_1 = 0$,

with maximum values given by $\left|\dfrac{g^0}{g^I}\right|_{max} = \dfrac{2}{b}$. The minima occur at frequencies given by

$\sin Q_1 = 0$ and the minimum amplifications are 2.

If $c < c_1$, then $b > 1$ and the maximum amplifications occur when $\sin Q_1 = 0$ and the maximum amplifications are 2. The minima occur when $\cos Q_1 = 0$ and have values of

$$\left|\frac{g^0}{g^I}\right|_{min} = \frac{2}{b}.$$

Figure 4.12 is from Haskell's paper and shows the amplification of planar SH-waves as a function of incidence angle (0 is vertical incidence). Amplification is given relative to a half-space which always has a free-surface amplification of 2. The model is layer of average crustal properties over a half-space with average upper mantle properties.

$$\begin{aligned}
\rho_1 &= 2.869\,{}^g\!/_{cm^3} \\
\beta_1 &= 3.635\,{}^{km}\!/_{sec} \\
h_1 &= 37\,km \\
\rho_2 &= 3.337\,{}^g\!/_{cm^3}
\end{aligned} \tag{4.94}$$

For vertical incidence, you can see that the maximum amplification occurs at periods given by

$$T_n = \frac{4h}{(2n-1)\beta} \qquad n = 1, 2, 3, \ldots \tag{4.95}$$

which is identical to the modal frequencies obtained from the plate with a rigid bottom in (4.68).
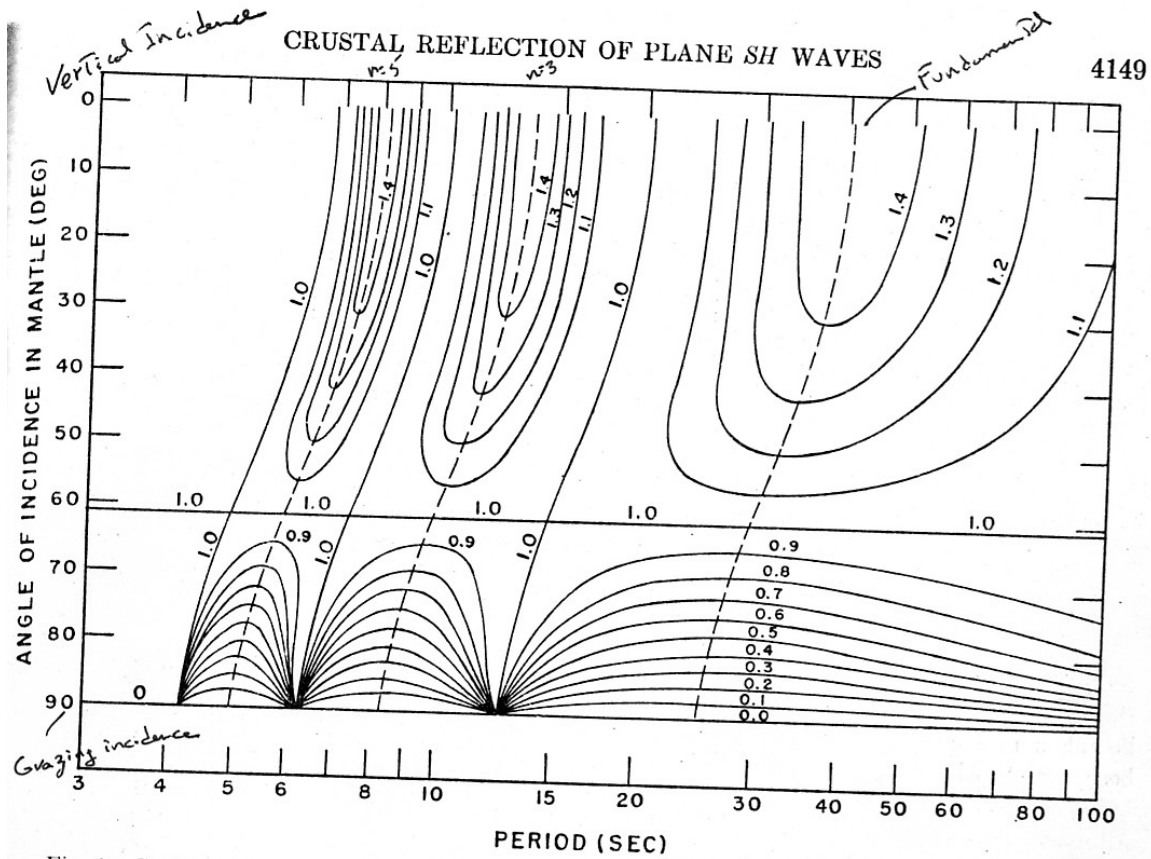

Figure 4.10 Amplification of SH-waves relative to a half-space as a function of incidence angle and period of a harmonic SH-wave incident on the crust. From Haskell (1960).

For vertical incidence the maximum amplification at these frequencies is simply

$$\left| \frac{g^0}{g^I} \right| = \frac{\rho_2 \beta_2}{\rho_1 \beta_1} \tag{4.96}$$

Whereas the maximum amplification of an SH-wave transmitted across an interface is 2 (see equation(4.25)), the maximum amplification of a harmonic wave can be very large at certain frequencies if there is a very low velocity layer over a half space.

San Francisco Bay Mud

Propagator matrix solutions are very important for analyzing problems where there is a layer of very low velocity material overlying a much higher velocity material. One of the most dramatic examples of this is on the margins of the San Francisco Bay where pporly consolidated Holocene mud deposits overly crystalline rocks. The following figure sre from "Analysis of seismograms from a downhole array in sediments near San Francisco Bay" by Joyner, Warrick and Oliver (1970, BSSA, 60, 937-958). Figure 4.11 shows the location of a 186-m deep borehole adjacent to the Dumbarton Bridge.
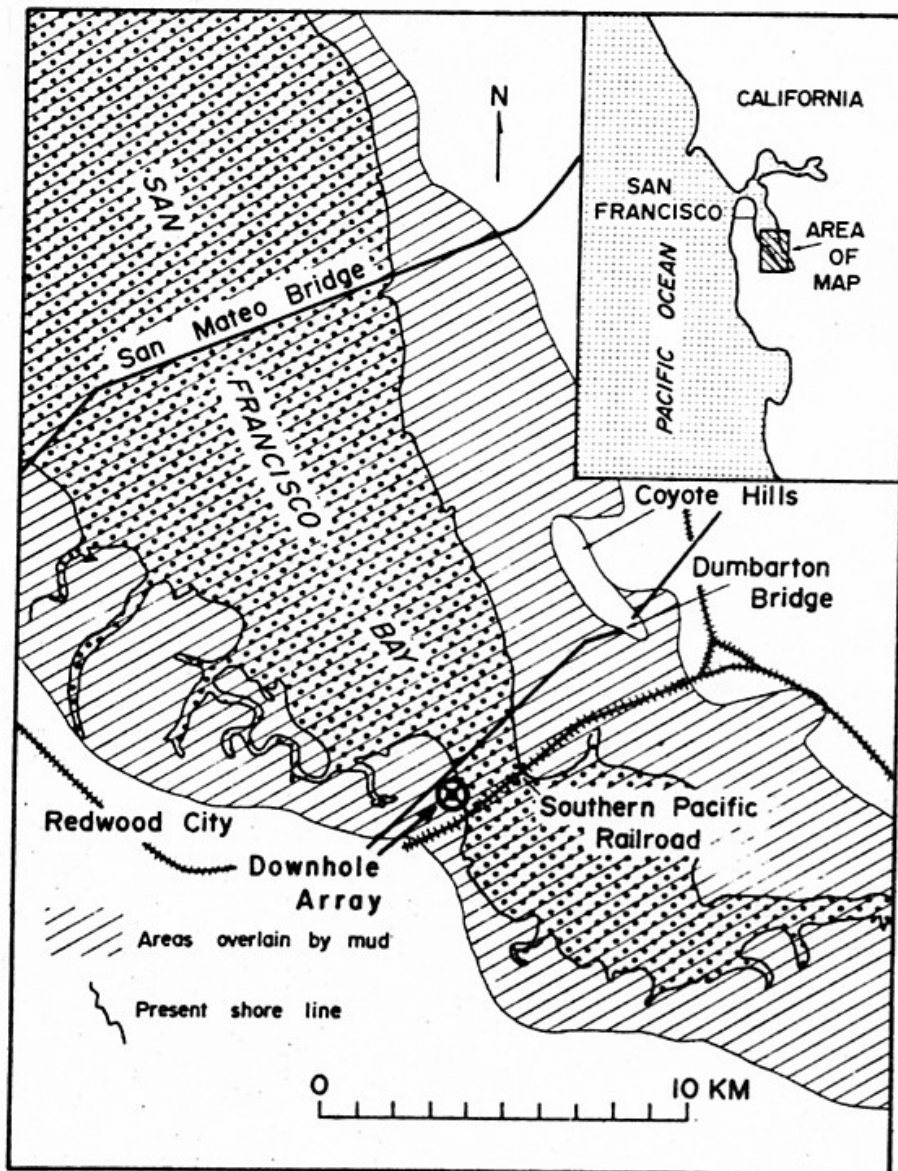
Figure 4.11 Map of southern part of San Francisco Bay showing location of the borehole. From Joyner and others.
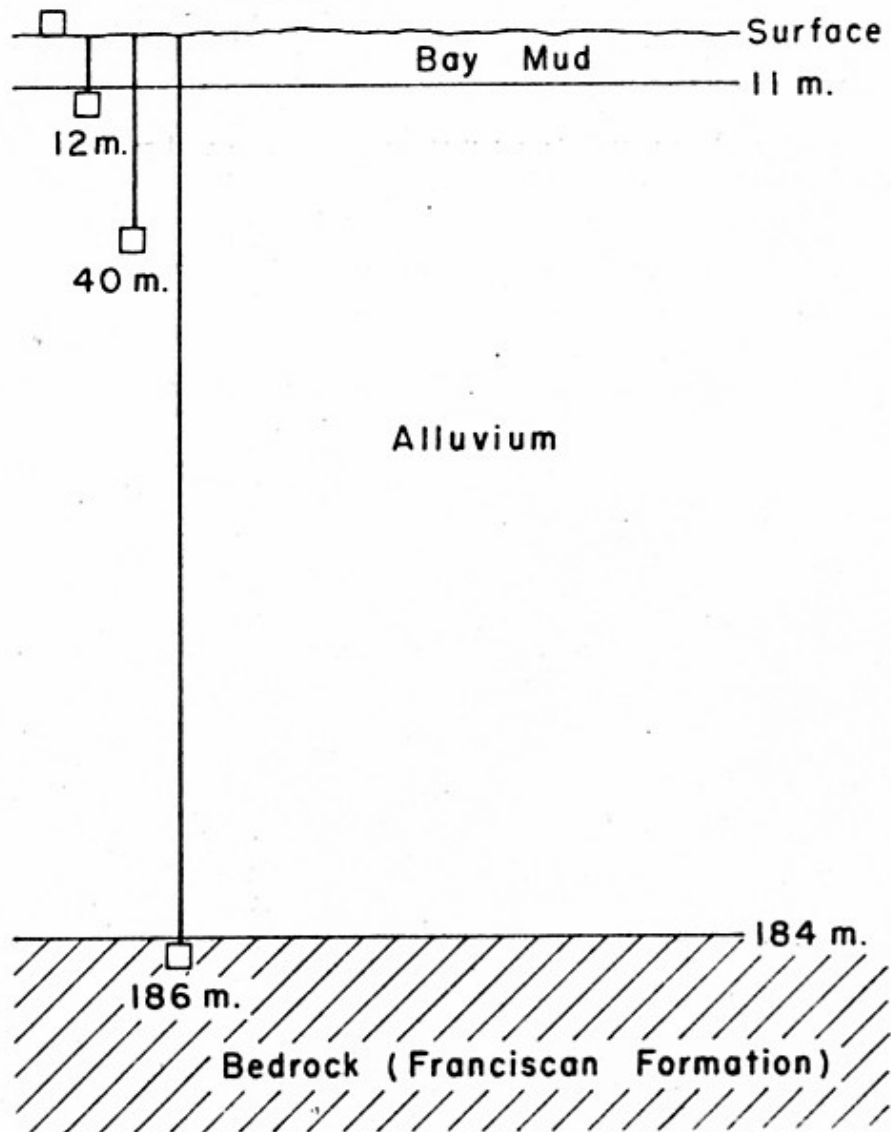
Figure 4.12 Schematic of the locations of seismometers in the borehole. From Joyner and others

Four 3-component sets of velocity-transducer seismometers with natural periods of 4.5 Hz were installed at depths of 0, 12, 40, and 186 m below the surface. The Bay mud is a Holocene mud whose mass is 50% water. The Alluvial deposits are though to be Pleistocene.

Figure 4.13 show the estimated S-wave velocity in the borehole and Figure 4.14 shows the seismograms from different levels for a M3.1 earthquake. Notice that not all of the channels were working However, as we would predict from the wave propagation discussion in this chapter, the signals are much larger at the surface than they are at the bottom of the hole.
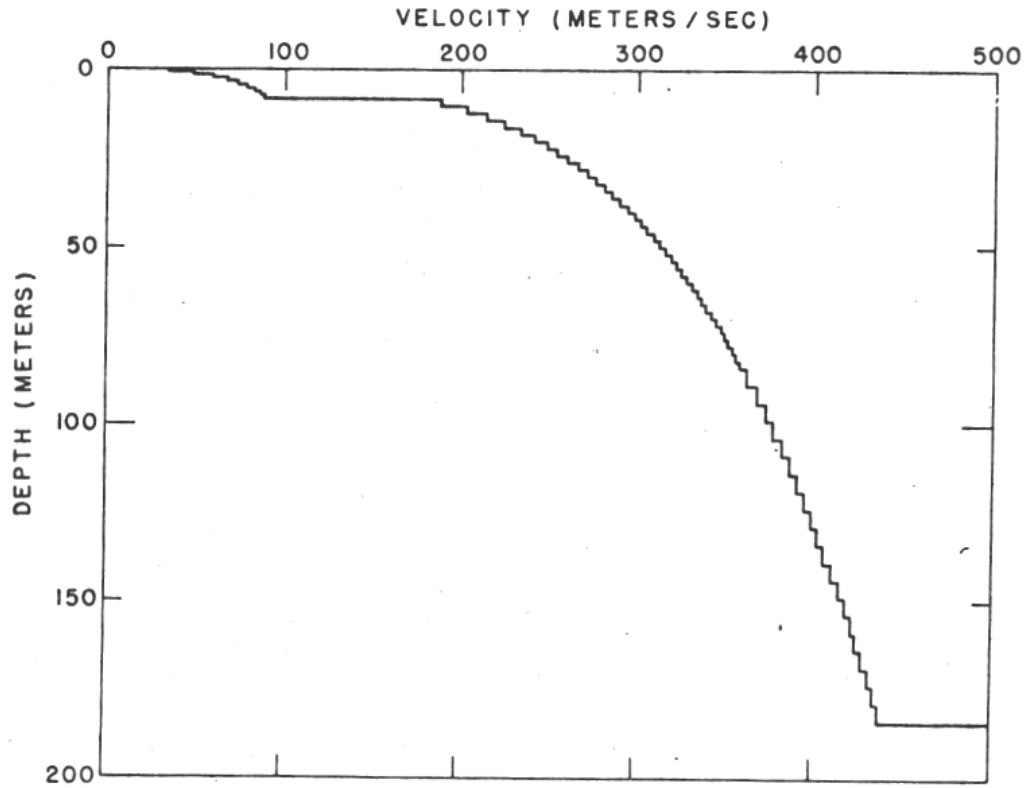
Figure 4.12 Shows an estimate of shear-wave velocity as a function of depth. The velocity model was developed by a combination of seismic travel-time data and from other studies of the properties of bay mud. The velocity in the bedrock is 2200 m/sec. From Joyner and others.
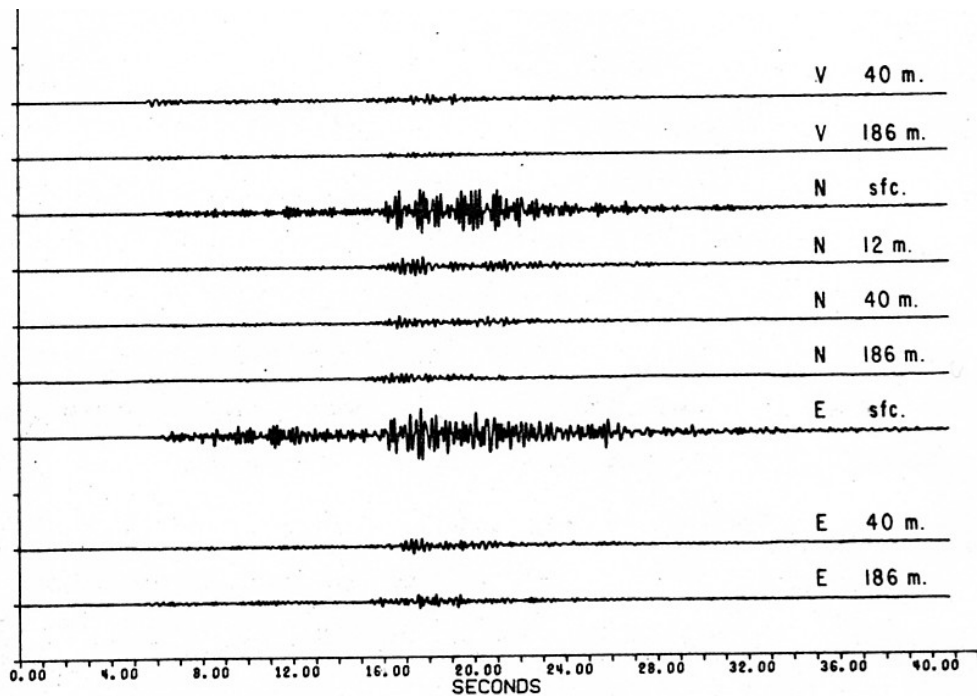

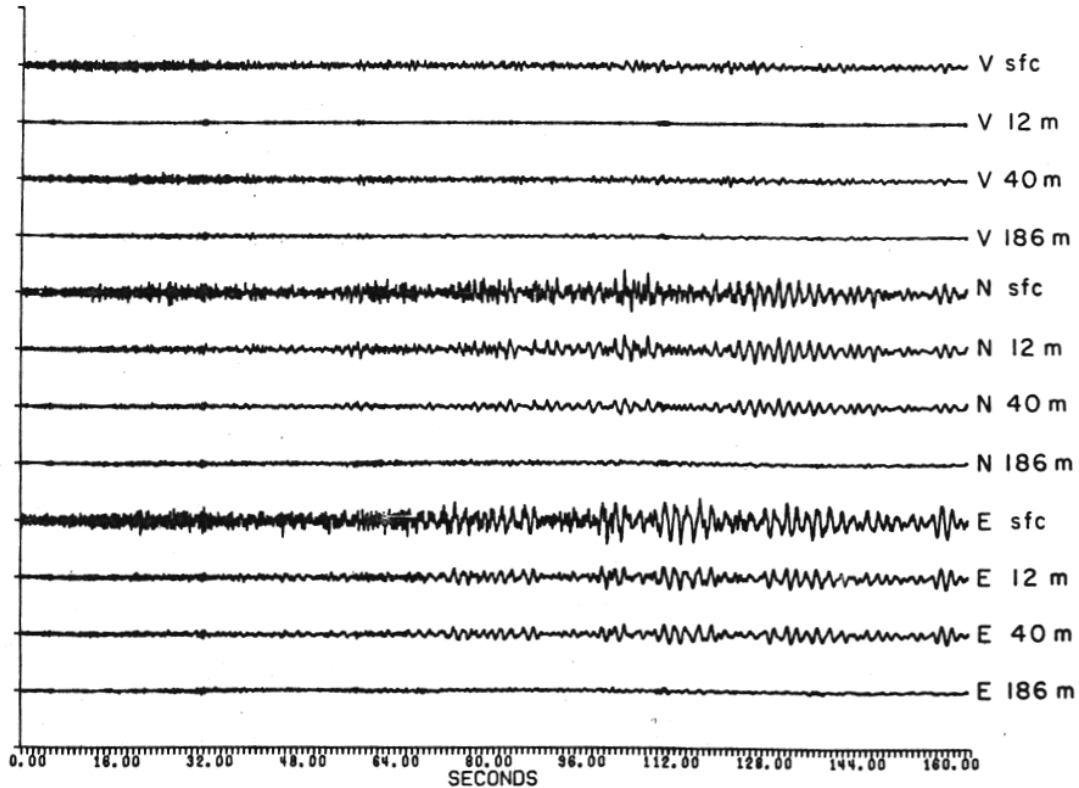Figure 4.13 Seismograms from a M 3.1 at a distance of 79 km.

Figure 4.14 Seismograms from the 1971 M 6.7 San Fernando earthquake at a distance of 485 km. From Joyner and others. Notice the harmonic nature of the seismograms from the shallow sites. This is caused by resonance of vertically propagating S-waves.

There are actually several resonance periodicities that we expect since there are two strong velocity contrasts; one at the mud-alluvium interface (11 m) and another at the alluvium-bedrock interface (180 m). The velocity of the bay mud averages about 70 m/sec (150 mph) (velocity of sound in air is 330 m/sec). Equation (4.95) tells us that we expect to see amplification at frequencies of about 1.6 Hz, 4.8 Hz, etc. for the mud layer. The alluvium layer is thicker faster, but much thicker and it has a resonance somewhere near 0.5 Hz.

The mud resonance can be seen in Figure 4.15 where the ratios of the Fourier amplitude spectra of the seismometers at the top and bottom of the mud are shown for a M3.6 earthquake. Also shown are predictions of these amplifications using Thompson-Haskell propagator matrices and the velocity model shown in Figure 4.12. The computations were performed for several different values of attenuation Q.

The resonance of the overall soil-mud column with the bedrock is shown in Figure 4.16, where the spectral ratio of the surface vs. the bedrock is shown for the 1971 San Fernando Earthquake. Spectral ratios are shown for different segments of the record.

Finally, Figures 4.17 and 4.18 show the basement and surface ground motions along with the ground motion assuming that most of the motion is due to vertically propagating S-

4-30

waves, and that this motion can be computed using propagator matrices to "propagate" the motion from the basement to the surface.
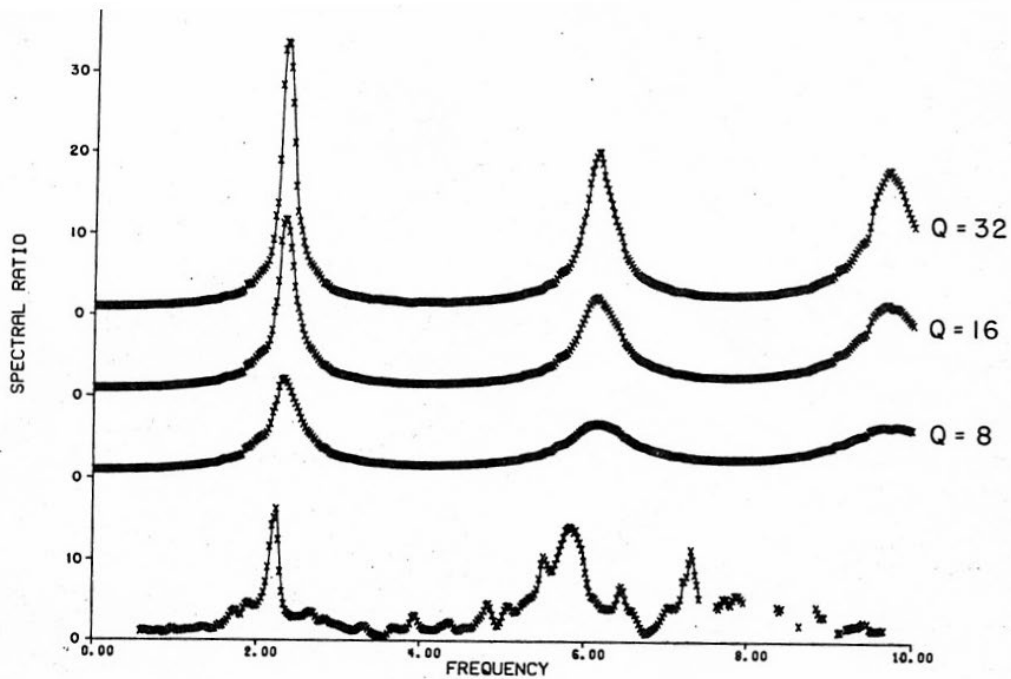

FIG. 7. Horizontal spectral ratios between the surface and 12 m. The *bottom curve* gives the observed ratio for the north component from the Pittsburg earthquake (magnitude 3.6, distance 66 km). The *other curves* give the predicted ratios computed for the model described in the text with different values of Q assumed for the material above 8 m.
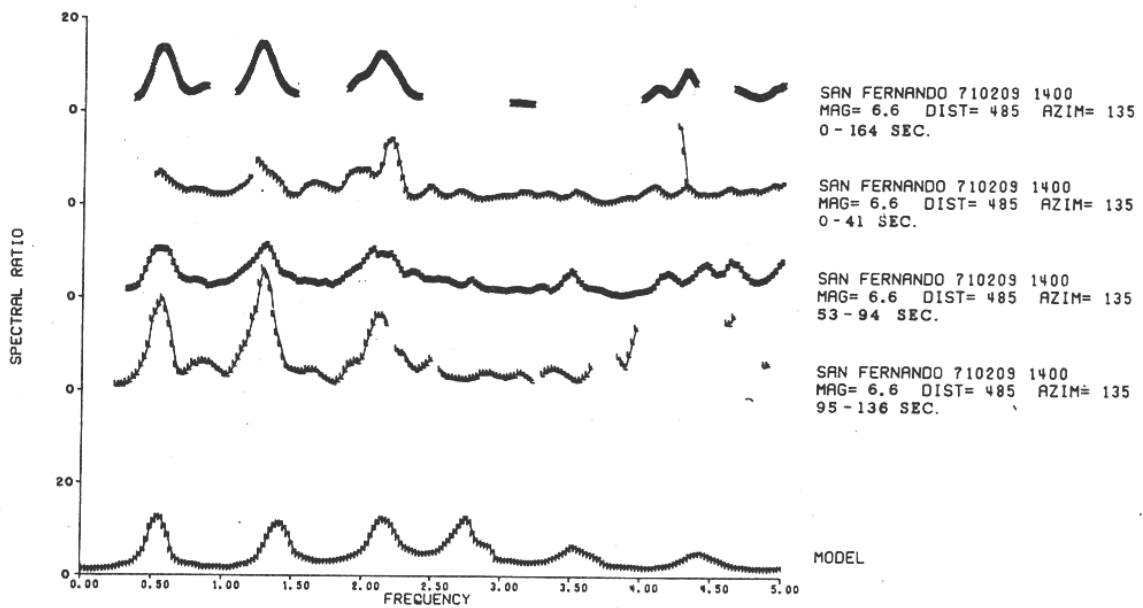
Figure 4.15 from Joyner and others.

FIG. 9. Horizontal spectral ratios between the surface and 186 m. Computed ratio for the model is compared with observed ratios for the north component from different segments of the record of the San Fernando earthquake, as described in the text.
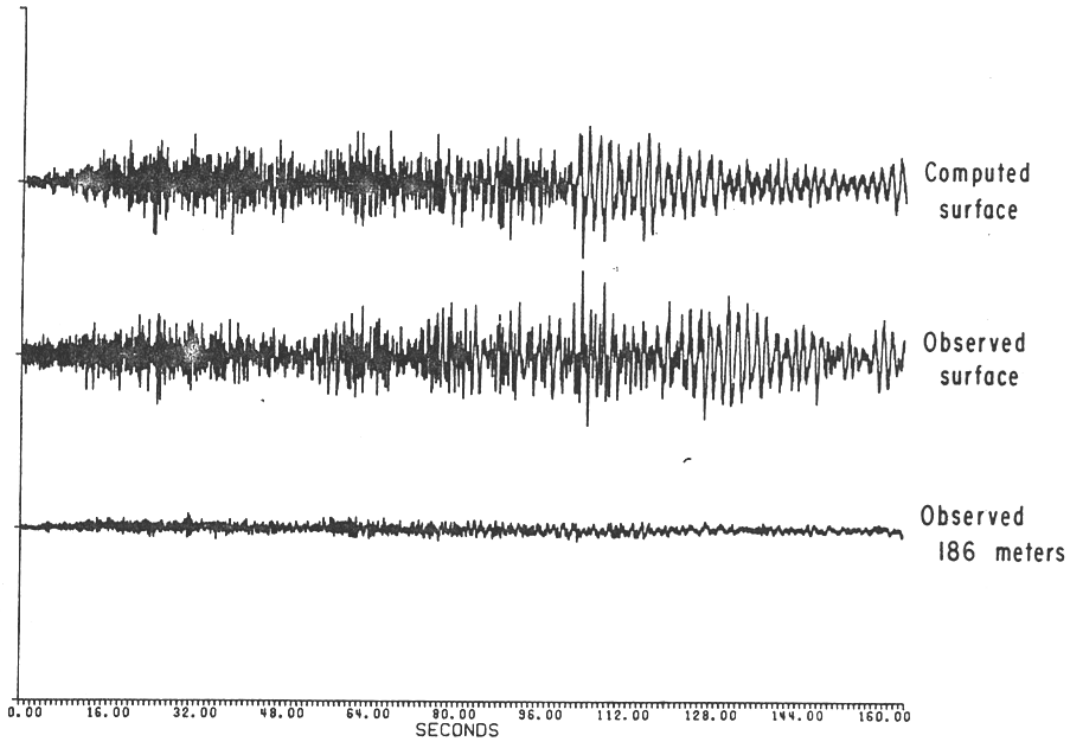
Figure 4.16 from Joyner and others

4-31

FIG. 14. Comparison of computed and observed motion for the north component from the San Fernando earthquake.
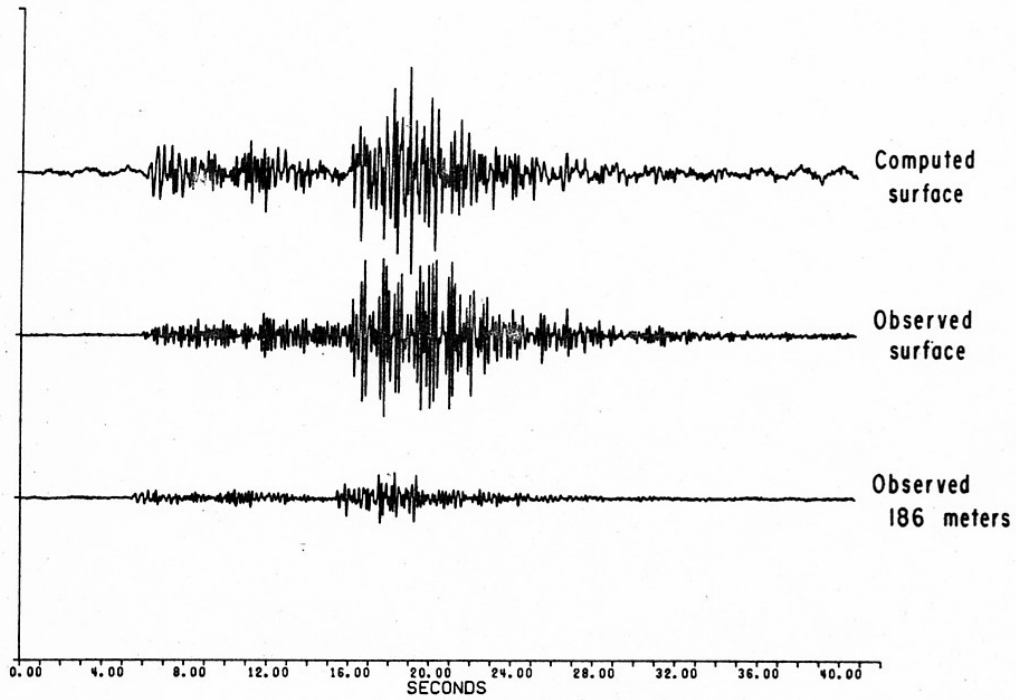
Figure 4.17 from Joyner and others

FIG. 16. Comparison of computed and observed motion for the north component from the Anzar earthquake (magnitude 3.1, distance 79 km).

Figure 4.18 from Joyner and others.

One of the most famous of all soil resonances occurred in the soft sedimentary lake deposits on which Mexico City is built. These deposits have S-wave velocities of about 80 m/sec and thicknesses of about 50 m. Figure 4.19 shows acceleration records from the 1985 Michoacan earthquake (M8.2). Notice how much larger the accelerations were in the sites in Mexico City.
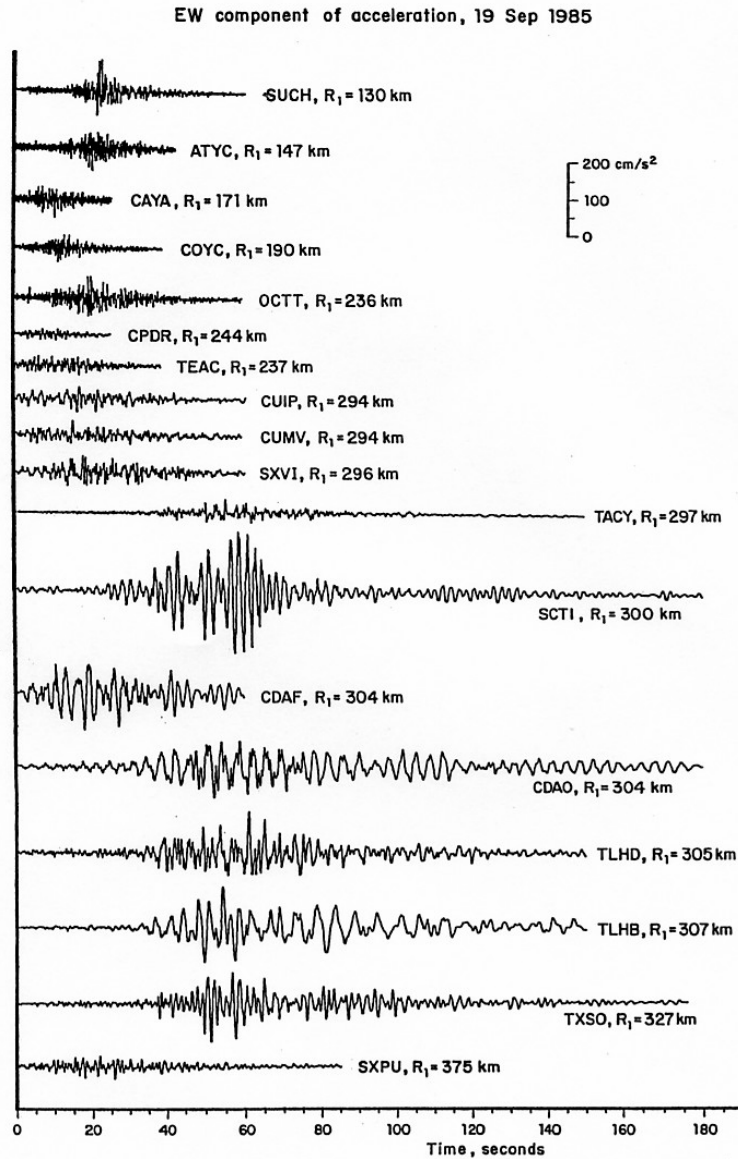
EW component of acceleration, 19 Sep 1985

Figure 3 East-west component of acceleration from the 19 September 1985 Michoacán, Mexico, earthquake from selected sites. Records are shown in order of increasing distance from the rupture area. Sites CUIP, CUMV, SXVI, TACY, SCT1, CDAF, CDAO, TLHD, and TLHB are all in Mexico City. Note the variation in ground-motion characteristics for this earthquake (from Singh et al 1987; copyright Seismological Society of America).

4-33

Homework

4-1. Show that the reflection and transmission coefficients match the boundary conditions for an incident planar SH wave onto the interface between two Poissonian solids.

4-2. Write the vector solution for an incident planar SV wave onto the interface between two Poissonian solids. This is similar to equations (4.29) and (4.30).